8-2001

Determination of Threshold Velocity and Entrainment Rates from a Copper Tailings Pond

Fook-Chi Soo
University of Tennessee, Knoxville

To the Graduate Council:

I am submitting herewith a thesis written by Fook-Chi Soo entitled "Determination of Threshold Velocity and Entrainment Rates from a Copper Tailings Pond." I have examined the final electronic copy of this thesis for form and content and recommend that it be accepted in partial fulfillment of the requirements for the degree of Master of Science, with a major in Environmental Engineering.

Wayne T. Davis, Major Professor

We have read this thesis and recommend its acceptance:

Terry L. Miller, James L. Smoot

Accepted for the Council:
Carolyn R. Hodges

Vice Provost and Dean of the Graduate School

(Original signatures are on file with official student records.)

To the Graduate Council:

I am submitting herewith a thesis written by Fook-Chi Soo entitled "Determination of Threshold Velocity and Entrainment Rates from a Copper Tailings Pond". I have examined the final copy of this thesis for form and content and recommend that it be accepted in partial fulfillment of the requirements for the degree of Master of Science, with a major in Environmental Engineering.

Wayne T Davis

Dr Wayne Davis, Major Professor

We have read this thesis and recommend its acceptance:

Terry Miller

Dr Terry Miller

James Smoot

Dr James Smoot

Accepted for the Council:

Interim Vice Provost and
Dean of the Graduate School

Determination of Threshold Velocity and Entrainment Rates from a Copper Tailings Pond

A Thesis
Presented for the
Master of Science Degree
The University of Tennessee, Knoxville

Fook-Chi Soo
August 2001

DEDICATION

This thesis is dedicated to my parents

Mr. Kam-Chuan Soo

and

Mrs. Molly Soo

who have provided me with so much in life and continue to do so.

ACKNOWLEDGEMENTS

This page would not be enough for me to acknowledge everyone I would want to acknowledge. However, there are a certain few who stand out in the crowd. First and foremost, I would like to thank my advisor, Dr. Wayne Davis, who has been extremely supportive and patient with me throughout my career as a student in the department. I would also like to thank the faculty and the staff of the Civil and Environmental Engineering Department for making my stay here at the university a memorable one.

Lastly I would like to thank my brother, Fook-Wai Soo, who has endured and kept me sane throughout my course of writing this thesis, and most of all, for being a brother.

ABSTRACT

Wind erosion is a phenomenon that has plagued many people for centuries. There are many sources for wind erosion, such as agricultural farmlands, deserts, coal piles and mining areas.

Significant research has been conducted on wind erosion, especially on paved and unpaved roads, construction sites and quarry areas. Open storage coal piles have also been a target for wind erosion studies, as a lot of power plants burn coal to produce power. However, this study does not include any of the sources mentioned above. This study involves wind erosion from a copper tailings pond of a closed down copper mining and smelting operations facility. The tailing pond has dried up over the years leaving behind a pond of dried up tailings that looks like a desert. One particular site that had such a problem was the iron mine located in Northern Michigan. Winds of up to 60 km/hr resulted in a dust storm that reduced visibility to less than 1 meter in some places (Tailings and Mine waste 1998).

This study was conducted to determine the threshold velocity for entrainment of the tailings by the wind and also the effects of moisture on the entrainment rate of the tailings. The experiment was performed in a wind tunnel with a height of 30 cm, width of 10 cm and total length of 250 cm.

Table of Contents

Chapter

List of Tables

Table

List of Figures

Figure

Nomenclature

P	Erosion potential function
P_i	Erosion potential corresponding to the observed (or probable) fastest mile of wind for the i-th period between disturbances, g/m^2
R^2	Coefficient of correlation
k	Particle size multiplier
r	Particle radius, mm
u	Threshold velocity, m/s
u^*	Friction velocity, m/s
u_t^*	Threshold friction velocity, m/s

Chapter 1

INTRODUCTION

Wind erosion is a serious matter when it comes to agricultural land. The topsoil is the important part of the land as it is the most fertile. If this part of the land gets eroded, farmers are in great danger of losing their livelihood. Other concerns for wind erosion are the pollution that it poses to the general public and the potential for jeopardizing the sustainability of the land. One example is the ongoing project in Europe where there are four countries, Germany, Netherlands, Sweden and United Kingdom, which are involved in the WEELS study (www.geog.ucl.ac.uk/weels). WEELS stands for Wind Erosion on European Light Soils. The area of each of the sites used in the WEELS study is large, consisting of 25 km^2.

Particulate matter less than 10 μm aerodynamic diameter is a cause of major concern as these particulates may be inhaled into the human lungs and tend to be deposited (Chow, 1997). However, not all entrained dusts are small. Some are large and settle over short distance from where they were first entrained. Others can travel over huge distances such as the transport of desert sand from the Sahara Desert to the Continental United States.

The primary objective of this study was not to quantify the transport but instead to determine the threshold velocity and how moisture affects the threshold velocity. The second objective was to determine the entrainment rates and how moisture played a role in the reduction of entrainment of the particles.

The material that was used for this study was tailings from a copper mining and floatation facility that has been closed for a number of decades. What was left behind is a

pond of dried up copper ore tailings that used to be sludge waste from the refining process. The site looks like a miniature desert, with a barren sandy appearance. Occasionally, wind blown dust clouds have been observed at the site. However, during frequent trips to the site (once and sometimes twice a week) during the yearlong period of this study, no occurrences of this type were observed.

Chapter 2

LITERATURE REVIEW

The focus of this chapter is on the science of wind erosion and research that has been conducted in the field and the conclusions reached in those studies.

Wind erosion is an age-old occurrence that has caused many problems for mankind. Some of the more severe problems include the loss of agricultural land, the transport of Saharan Desert to the Americas, desertification and many more. The problem with the study of wind erosion is that each site has different characteristics and no one site is universal. Other factors that come into play in wind erosion are the weather patterns, terrain, vegetation, humidity and the characteristics of the surface materials.

Wind erosion occurs when the air pressure that acts on the soil is sufficient to overcome the gravitational and cohesive forces resisting particle detachment (Bagnold, 1941). There are a number of factors that affect the degree of a wind erosion event. These factors include surface roughness, topography, moisture content of the soil and the intrinsic properties of the soil itself.

Particle detachment by wind erosion has been identified as a two-stage event (Bagnold, 1941). The first stage is the static threshold where the direct action of wind causes detachment and the second stage is the dynamic threshold where stationary particles are bombarded by moving particles. Figure 2.1 illustrates this particular occurrence.

Sokolov was the first to establish that there were three types of grain movements: (1) rolling of particles along surfaces; (2) particles that break away from the surface and

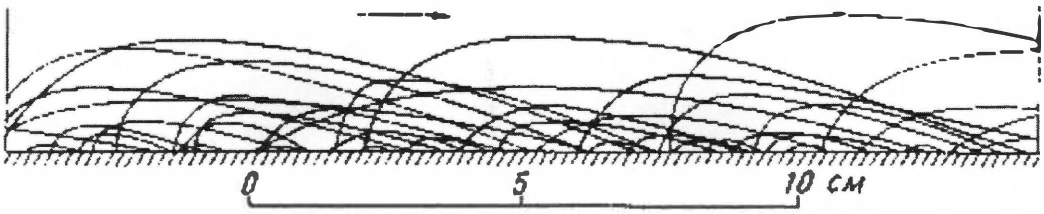

Figure 2.1. Particle Saltation

(Fuchs, 1964)

then fall back down (jumping movements) and, (3) particles that remain airborne after initial separation from surface, as depicted in Figure 2.2 (Fuchs, 1964). Research conducted by Bagnold, and later by Chepil, confirmed the three-stage event of wind erosion stated above (Fuchs, 1964). The research that was conducted by Bagnold involved a 30 cm × 30 cm wind tunnel with glass walls and mean velocities up to 0.10 m/s. From the research, it was found that many of the particles behaved in a manner described in Figure 2.1. It is obvious from the figure that many of the particles jump upwards almost vertically and then fall back down at a less steep angle further downstream.

After a particle has fallen back down from its flight, it either bounces off the surface and goes on for another jump or it buries itself and imparts it momentum to other particles that are on the surface, which would either roll or jump. This transport mode then causes a chain reaction.

Chepil's research covered a wide variety of soils and the results obtained were similar to what Bagnold had observed (Fuchs, 1964). Chepil also found that many of the jumping particles rotate at high speeds (200-1000 rpm) indicating that they were initially rolling before they jumped. Sand particles having a radius of between 0.09 and 0.15 mm are four or five times more likely to be jumping than rolling. Sand particles having a radius of 0.2 to 0.3 mm will not jump if the wind speed is less than 10 m/s (22 mph) and 1 mm particles will not move at all. Further research found that soils erode most readily for particle sizes with a radius of between 0.05 to 0.07 mm, corresponding to a friction velocity, u^*, of between 3.6 to 4.0 m/s, measured at a height of 15 cm. Chepil also

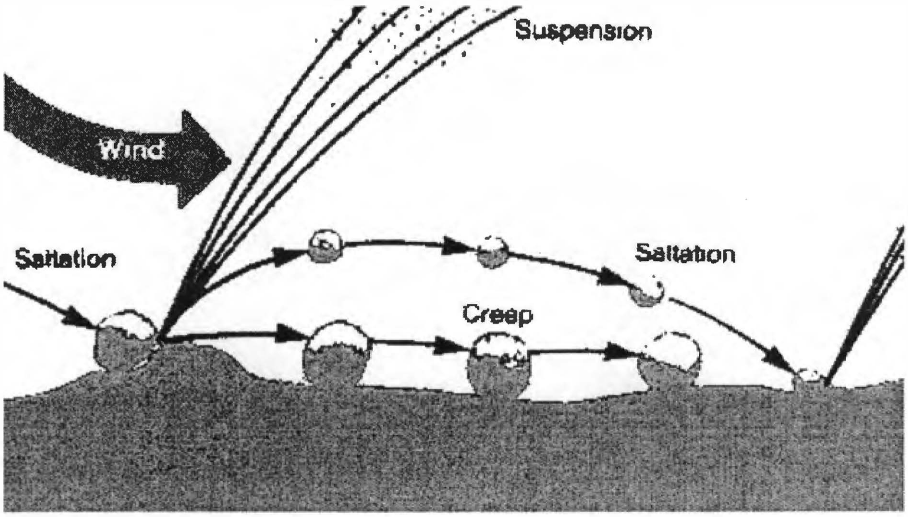

Figure 2.2. Three-phase Particle Movement

(http://www.qub.ac.uk/geosci/teaching/postgrad/workshop1/erosion4.html).

discovered that soils with radius less than 0.025 mm and sands with r > 0.5 mm hardly eroded at all due to the attractive forces between the particles (Fuchs, 1964).

Bagnold conducted experiments with sands of different dispersity and the results of his experiment are plotted in Figure 2.3. u_t^* is plotted on the ordinate axis against $\sqrt{r}$ on the abscissa, where u_t^* is the critical friction velocity and r is the radius of the particle. The solid continuous line I represents the dynamic velocity and II represents the static velocity, while the dotted lines are extrapolations. Two equations were derived from the graph and they are;

Dynamic $u_t^* = 164 \sqrt{r}$ cm/s (solid line I) (2-1)

Static $u_t^* = 208 \sqrt{r}$ cm/s (solid line II) (2-2)

The dynamic velocity is the velocity at which particles are moving as a result of bombardment from saltating and suspended particles. On the other hand, static velocity is the velocity at which that sand movement is caused only by fluid pressure. It was also found from the graphs that u_t^* was proportional to $\sqrt{r}$. An interesting point can be seen from the plotting of the static graph when $r < 0.05$ mm; the threshold friction velocity increases. This occurrence is due to the molecular forces between the particles. Contrary to popular believe, it is actually harder to get smaller particles suspended in the air due to the cohesive forces that are present between them. However, one has to keep in mind that this type of entrainment of particles is only due to the wind blowing and there are no external forces that come into play, such as disturbances from passing vehicles or livestock. Figure 2.3 shows that particle sizes of about 0.03 mm and smaller

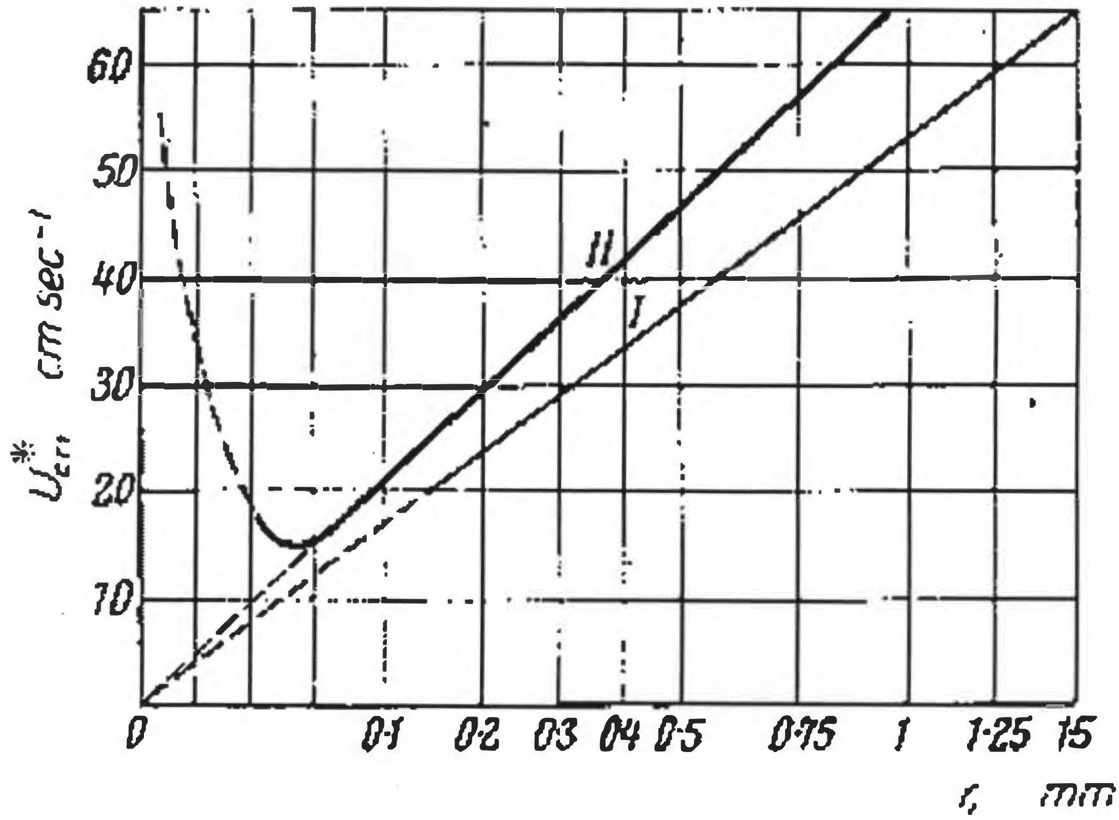

Figure 2.3. Fluid Threshold Friction Velocities

(Fuchs, 1964)

cannot be swept up individually after they have impacted because they sink into a layer of matrix of larger particles, out of reach of the turbulent air (Bagnold, 1941).

Bagnold observed that in the desert, particles with a mean radius of 0.12 mm had a threshold friction velocity of 0.23 m/s, measured at a height of 10 cm above the surface. Genzel produced a table, Table 2.1, that relates different particle sizes with their threshold friction velocities (Fuchs, 1964). Also included in the table is the threshold friction velocity for the same particle sizes, and the threshold friction velocity at two percent moisture content for the same size particles (Fuchs, 1964).

Table 2.1. Threshold Friction Velocity as a Function of Particle Size and Moisture Content

r, mm	0.087 - 0.12	0.12 - 0.25	0.25 - 0.5	0.5 - 1.0
u_t^*, cm/sec (dry sand)	380	480	600	900
u_t^*, cm/sec (sand with 2% moisture)	600	750	950	1200

From the table, it can be seen that there is an approximate proportionality of u_t^* to $\sqrt{r}$ for dry sand, thus confirming Bagnold's original finding of the proportionality. With two experiments showing similar results, it is then considered that the proportionality was well established.

In the EPA document AP-42, there is a chapter that discusses wind erosion. However, the discussion involves open storage aggregate pile, primarily coal overburden. Experiments that were carried out in the field, performed with a portable wind tunnel at a height of 15 cm above the surface, showed that threshold velocities were in excess of 5 m/s and particulate entrainment rates decay rapidly during an erosion event. An equation

was developed to determine the entrainment factor for wind generated particulate emissions from erodible and nonerodible surface material subjected to disturbance, in g/m^2-yr. It is given as:

$$\text{Emission factor} = k \sum_{i=1}^{N} P_i \qquad (2\text{-}3)$$

where k is the particle size multiplier, N is the number of disturbances a year and P_i is the erosion potential corresponding to the observed fastest mile of wind for the i-th period between disturbances in g/m^2. This emission factor is particle size and friction velocity related. Due to the difference of frequency in soil disturbance, each of the open storage piles subjected to erosion should be treated separately. The potential erosion equation that is used to determine the emission factor is given as:

$$P = 58 (u^* - u_t^*)^2 + 25 (u^* - u_t^*) \qquad (2\text{-}4)$$

$$P = 0 \text{ for } u^* \leq u_t^* \qquad (2\text{-}5)$$

where u^* is the friction velocity and u_t^* is the threshold friction velocity. Both velocities are measured in m/s.

Another reason why each of the erosion events has to be treated differently is because of the nonlinear form of the erosion potential equation. There are limitations to both the emission factor and potential equation erosion equation given in AP-42. They are limited only to dry and exposed surfaces with limited erosion material. Another is that the values are valid only to a time period of between disturbances of the surface. After the surface is disturbed, the erosion potential has to be recalculated, hence the N term in the summation. The N term is used with respect to daily disturbances, which means N can range from 0 to 365, because there are 365 days in a year. The N term does not take

into account the number of times the surface is disturbed in a day, just whether it is disturbed in a day or not.

Gillette (1980) noticed that there was very little field-tested information on threshold wind velocities for undisturbed and disturbed desert soils on which has the largest potential for erosion. Since that was the case, Gillette conducted a study to measure threshold velocities for a wide variety of natural desert surfaces to estimate the threshold velocities in terms of desert geomorphology. As one would expect, threshold friction velocity is affected by numerous factors in the field and the study attempted to relate threshold friction velocity to as many factors as possible, although there was no one single equation that was developed which incorporated the entire range of factors.

One of the first findings of the research was that soil moisture content is related to the amount of salt content; the higher the salt content, the higher the moisture content of the soil. This is because the high salt content inhibits the evaporation process and also preserves sufficient amount of moisture to inhibit entrainment. Also, salt crystallization binds particles together, further reducing the entrainment process. All of the soils tested by Gillette that had salt content over 1% were nonerodible. The second finding was the relationship of the thickness of the crust for undisturbed samples. All of the undisturbed clay samples with a crust thickness of at least 0.5 cm needed at least a friction velocity of 2.5 m/s in order for entrainment to occur. The equation developed for undisturbed sandy and gravelly soils is;

$$u_t^* = 48 + 59 \times \textit{Thickness} \quad R^2 = 0.68 \qquad (2\text{-}6)$$

The *Thickness* term is a measurement of crust thickness in centimeters and the resultant threshold friction velocity is in cm/s. The coefficient of correlation, R^2, stated above showed that the data correlated reasonably well, having a value of 0.68.

The third relationship that was developed is related to the aggregate size distribution. As noted by Gillette, the erosive tendencies of a soil are a reflection of the size of the largest fraction of the soil. Gillette came about this conclusion with the data collected by Chepil (1951). The data showed a definite trend of increasing threshold friction velocity with the larger mode of the aggregate size distribution, yielding an approximate relationship of;

$$u_t^* = 43 + 0.0093 \times \textit{Mode} \qquad R^2 = 0.68 \tag{2-7}$$

for disturbed soil samples and

$$u_t^* = 64 + 0.0055 \times \textit{Mode} \qquad R^2 = 0.64 \tag{2-8}$$

for undisturbed samples. Again the data related well with the equation developed. The *Mode* of the aggregate diameter is measured in micrometers and the resultant friction velocity is in cm/s. As mentioned previously, soil texture is one factor that can influence the threshold friction velocity of the soil. Gillette mentions that sand dunes (composed almost entirely of sand) have a threshold friction velocity of about 0.2 m/s. However, if the clay content of the soil is in excess of 20%, the threshold friction velocity exceeds 2 m/s (for undisturbed samples). The equation developed for undisturbed soils with less than 20% clay is;

$$u_t^* = 53 + 5.1 \times \textit{Silt percentage} \qquad R^2 = 0.73 \tag{2-9}$$

and the equation for which the clay exceeds 20% is;

$$u_t^* = 390 - 3.3 \times \textit{Sand percentage} \qquad R^2 = 0.72 \tag{2-10}$$

The equation developed for sand content greater than 90% is;

$$u_t^* = 14.5 + 0.0071 \times Mode + 1.59 \times Colloidal\ clay \quad R^2 = 0.77 \qquad (2\text{-}11)$$

Equations 2-8, 2-9 and 2-10 showed even better correlation with data compared to some of the previously developed equations. Some other variables that were found to have no significant affect on the soil are the pH, organic content and carbonate content.

An overall summary by Gillette in the experiments was that the highest correlation with threshold friction velocities was found by using the *Mode* of the dry aggregate size distribution. The relationships developed for the undisturbed soils state that the threshold friction velocities depend on soil mixture, with fine soils having high threshold friction velocities and sandy soils low threshold friction velocities. On the other hand, relationships that were developed for the disturbed soils state that the threshold friction velocity for finer pulverized soils is lower and for coarser-pulverized soils with high fine clay content the threshold friction velocity is higher.

There is a second factor that is involved the wind erosion process, the wind itself. When air moves over a solid surface, a boundary layer develops between the two in which the surface retards the flow of the air. There exists a velocity gradation, from zero velocity at the surface of the solid to a velocity where the flow is no longer affected by the frictional force of the surface in the boundary layer. The gradation of the flow of wind, with respect to the height above ground, produces a velocity gradient that in turn produces shear within the boundary layer (Bagnold, 1941).

If the velocity of air beyond the boundary layer is stable, then laminar flow may occur. If the flow is indeed laminar, then it is most likely to happen only close to the surface where the flows are very slow. However, under normal conditions, the airflow is

not steady but gusty thus causing the flow over the surface to be irregular. The irregular wind flow then causes turbulence, which also exhibits zero motion where the air meets the solid surface. With all the turbulence, the average velocity of the turbulent flow would still display an equilibrium velocity gradient as in the case of the laminar flow. However, in a boundary layer with turbulent flow along with a lot of mixing, the vertical gradient is steeper and the shear stress is greater (Bagnold, 1941). This phenomenon was observed from the theory that when the wind exceeds a certain critical strength, it changes from laminar flow to turbulent. The drag that arises from the flow of wind in the tunnel is then transferred to the wall not by individual molecules but instead by the momentum of the eddies of flow. This then causes the drag force to vary with the square of the velocity.

From Bagnold's study of the wind gradients, there is an obvious difference of velocity with respect to the difference of height from the surface. The two lines presented in Figure 2.4 were velocity traverses taken at different heights above the surface of the wind tunnel. The results were plotted in a log-linear graph to illustrate the relationship of wind velocity with respect to height, mentioned previously. As a matter of fact, the relation that Bagnold found was that the velocity is proportional to the logarithm of the height above the surface, as illustrated in Figure 2.4. One of the reasons why the graph was plotted on log-linear axis is because the linear-linear axis graph has a curved shaped graph that is hard to analyze. Both of the lines intersect the y-axis at the point of approximately 1.5 mm. Further analysis with different velocities showed that not all of the velocities intersect at this point but instead they converge at a height of

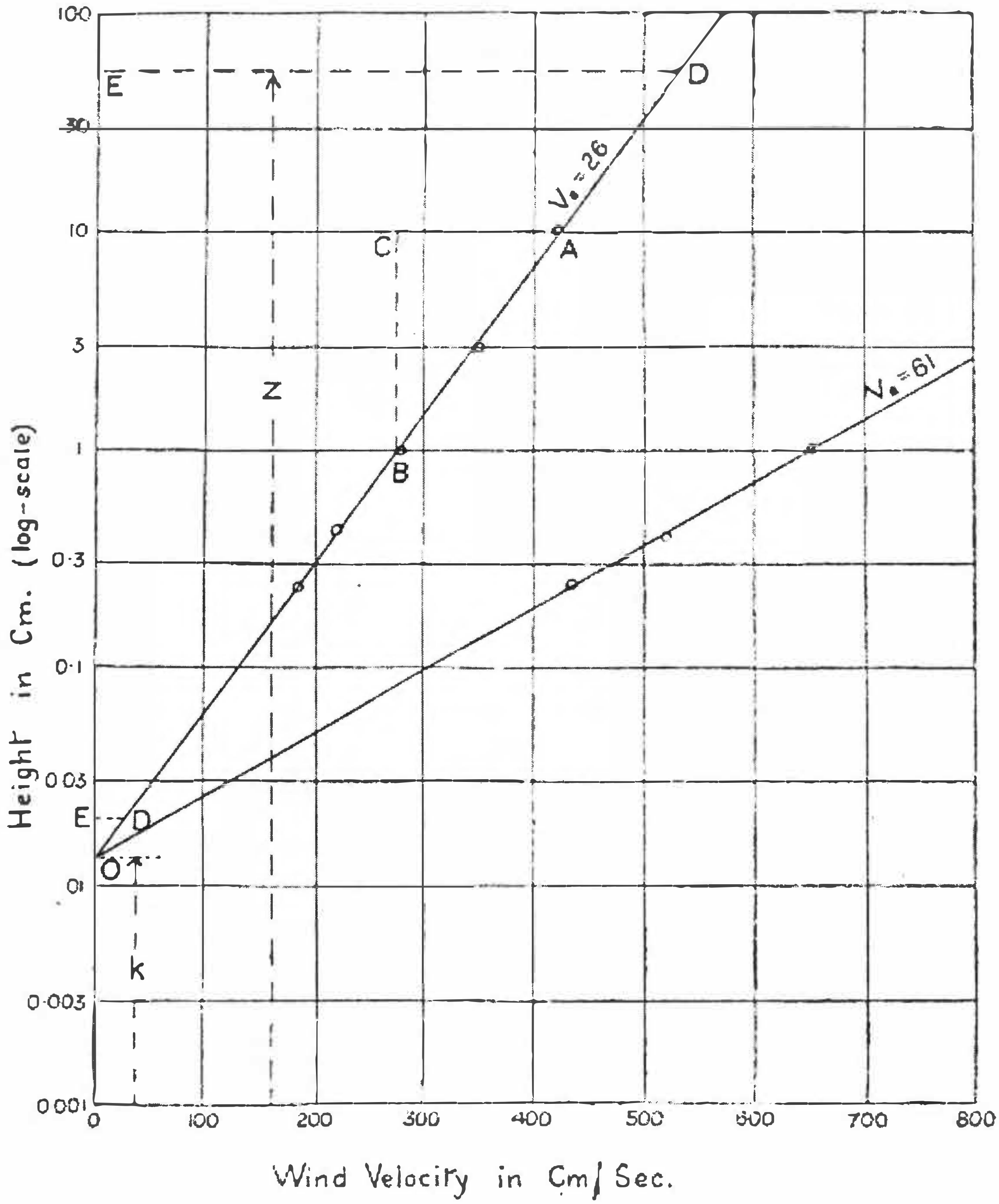

Figure 2.4. Illustration of wind velocity measurement at different heights above the surface (Bagnold, 1941).

3 mm above the ground. This phenomenon showed that no matter how fast the wind is blowing, the wind velocity remains the same at about the height of 3 mm from the surface. Moreover, it was also discovered that the velocity actually decreases closer to the surface. This was the one of supporting pieces of evidence that was used by Bagnold to develop the idea of the three-phase particle movement theory.

One other factor that was not addressed here is the effect of freeze drying has on the tailings. On November 16, 1996, a dust storm event that reduced visibility in the surrounding areas of two surface iron ore mines in Upper Peninsula, Michigan (Price, Vashers, Vitton, Paterson, 1998) to less than 1 meter prompted Cleveland Cliffs Incorporated (CCI) to take action in an effort to make sure that such an occurrence would not again come to pass. These mines are unique in a way their milling process produces tailings that are generally less than 20 μm in diameter. This is a matter of concern as EPA regulates any particulates that are less than 10 μm in diameter. The dust storm event was a result of 60 km/hr winds coupled with cool dry conditions of the tailings pond. The freeze drying phenomena happens when the water in the pore spaces of the tailings freezes and then sublimates directly to the vapor phase. This in turn produces tailings with no cohesion, thus very susceptible to wind erosion. However, the study does not mention what velocity is sufficient for erosion to occur.

Chapter 3

MATERIALS AND METHODS

The laboratory experiments conducted in this study involve determining the threshold velocity of the tailings and entrainment rates of the tailings when exposed to different velocities for different time intervals and at different moisture conditions.

3.1 Description of Tailings

Tailing samples were obtained from the tailings pond at the site. The composite tailings were taken from different locations within the pond in order get a representative sample. A sieve analysis was performed in the laboratory to determine the distribution of the tailings. The sieve analysis not only provided a better understanding of the distribution of the tailings but also the basis for classification of the tailings. Results of the sieve analysis can be seen in Figure 3.1. Using the Unified Classification System, ASTM D-2487-69 (Cernica, 1995) the tailings can be classified as sand-clay mixtures (SC). This means that the tailings are mostly sand with a mixture of clay.

Two different samples were taken because it was assumed that the top half inch of the tailing is essentially what is getting blown off-site and the second sample, taken up to a six inch depth, was analyzed due to its potential to get eroded. Both of the samples exhibited similar distribution of particles. Although both samples showed similar distribution of particles, they both had significantly different moisture contents. The top half-inch of the sample only had approximately only 0.3 % moisture content while the

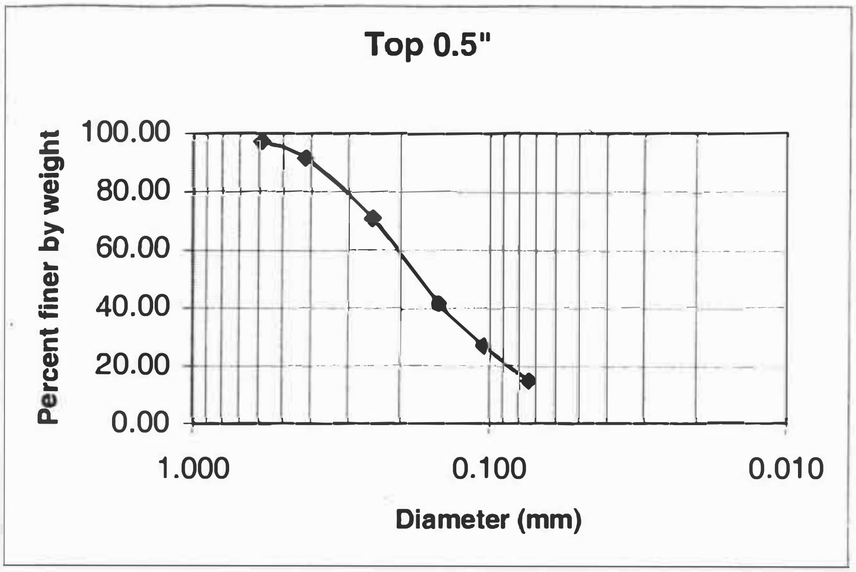

a. Sieve analysis on the top half-inch of the tailings.

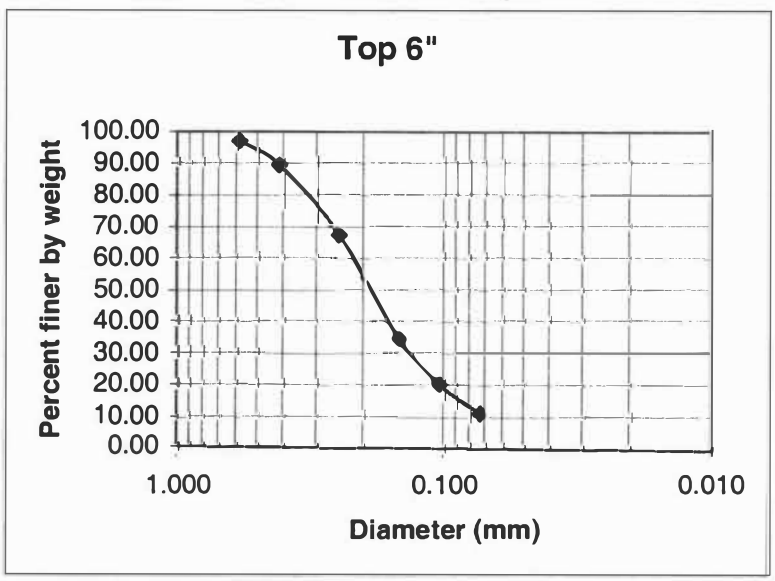

b. Sieve analysis on the top six-inch of the tailings.

Figure 3.1. Sieve Analysis on the Tailings Collected

bottom five inches had about 7% moisture. This may not really matter if both samples are dried prior to use. The top half-inch tailings were chosen for use in this study over the top six-inch tailings for the experiments because it had less moisture content and therefore dried faster in the oven and was more readily available for entrainment in the field.

After drying the sample and performing the sieve analyses, it was determined that an Optical Particle Counter, which was originally intended to be used to measure the entrainment of particles, was not able to measure the amount of tailings that were going to be entrained into the air stream in the wind tunnel. This is because the OPC provides a measurement of the number of particles in the air stream for particle sizes from 0.3 μm up to 8 μm, whereas the total amount of tailing that passed the 200-mesh sieve (75 μm opening) was less than 15%, on both of the sieve analysis performed. This would mean that the OPC would not be able to measure the larger particles that get entrained into the air stream. It was then determined that a gravimetric means of determining particle loss due to entrainment would be a better approach than trying to count particles.

3.2 Experimental Procedures

Both threshold velocity experiments and entrainment rate determination experiments were conducted. Threshold velocity is the velocity at which the particle is blown off the surface and entrains into the air. A schematic of the test stand and wind tunnel used for the experiments is provided in Figure 3.2. The system is composed of simple ductwork that has a fan on one end and is connected to the building ventilation

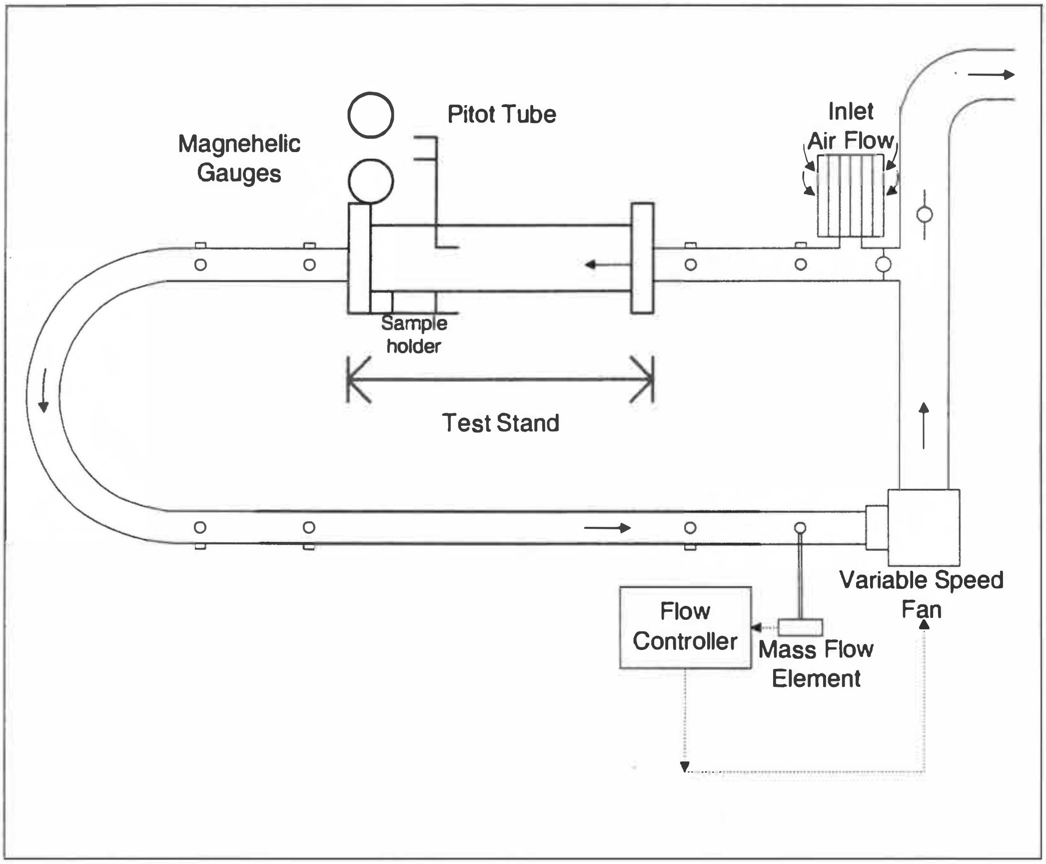

Figure 3.2. Schematic of the Test Stand with the Wind Tunnel

system at the other end. The fan is a variable speed fan, which allowed for the variable velocities.

In order to determine the threshold velocity of the tailings, the fan was turned up to a certain velocity and left there for five minutes. If there were no losses measured, then the threshold velocity of the tailings was not reached. This process was carried out at different final velocities until the threshold velocity was reached, except for one case where the threshold velocity was never reached (due to the high amount of moisture added). Tests were also conducted at higher velocities than the threshold velocity just to get an indication of the increased entrainment at higher velocities. It is only natural to expect higher losses at higher velocities. The resulting graphs are plotted and discussed in Chapter 4.

As mentioned in the introduction, the objectives were not only to determine the threshold velocity but also how moisture affects the threshold velocity. In order to determine the effect of moisture on the threshold velocity, dry tailings had to first be tested to get a reference point for the comparison. Then the wetted tailings were subjected to the same experiment. There were four different sets of wetted tailings that were tested. The dry tailings experiment required the tailings to be dried in the oven to remove any moisture that was absorbed while in the laboratory. On the other hand, for the wetted tailings experiment, the tailings were normalized to room temperature and humidity prior to use. This is because the oven-dried tailings have a temperature of 105 ^{o}C when first removed from the oven and any water that would have been added would have immediately been evaporated off the surface.

The entrainment rate experiments were conducted as follows. As in the case of the threshold velocity, a portion of the tailings was dried in the oven at 105 °C so that it had no moisture. Each of the tailing samples was left in the oven at least 24 hours prior to use to ensure that it was fully dried. This was done to determine the theoretical worse case scenario as dry tailings entrain the easiest. The tailings were transferred from the oven to a petri dish, with a diameter of 42 mm, and then weighed on a scale. As the petri dish was not able to withstand the heat in the oven at 105 °C, it was not inserted into the oven with the tailings, which would have been the ideal situation because there would have been minimal loss of tailings from the transferring of material. After weighing the petri dish and sample, the sample was then taken to the wind tunnel. In all tests, the tailings used were the top half-inch tailings. Each tailing sample was then exposed to a specific wind speed for a predetermined amount of time to quantify the loss associated with the wind velocity. The values obtained in this part of the experiment are later corrected for ramping losses, which are discussed later.

After exposing the tailing sample in the wind tunnel for a specific velocity, it was then weighed again to determine how much of the tailings were lost. The amount lost is then plotted against the time of exposure. Based on the assumption that the results were going to vary over a range, it was decided that multiple runs had to be performed for each velocity data point to get an average value. Each of the data points on the velocity graphs presented in Chapter 4, with the exception of the threshold velocity graphs, were results of an average of eight runs.

The second part of the laboratory entrainment rate experiment involves spraying some water on to the surface of the sample to simulate a rain effect and/or a morning dew

effect. The average amount of water that was added to the tailings was less than 1% of the total weight. The addition of the moisture was just on the surface, not evenly distributed throughout the entire depth of the petri dish. This was done in order to preserve the amount of fine particles that were present. If the tailings were to be mixed according to ASTM standards, many of the fine particles would have been lost. This procedure not only preserves the fine particles, it was intended to simulate real world rain and/or morning dew events.

The use of 'moisture content' in conventional terms in this context is therefore incorrect due to the unevenly distributed moisture in the tailings. Instead, the amount of moisture added was to be reported in terms of rainfall, i.e. in cm, similar to the reporting of rainfall events.

After the tailing sample is inserted into the wind tunnel, a fan has to be turned on to get the desired wind velocity. In order to get the desired velocity, the fan has to accelerate from a stand still to the desired velocity. The acceleration phase of the fan will cause some of the tailings to be blown off into the air stream. Therefore, if the time measurement was to start at the same time the fan started, it would be hard to quantify how much was actually blown off in the acceleration phase and the actual constant velocity phase. In order to overcome this problem, a series of tests were initially conducted in which the tailings were placed into the wind tunnel and the fan was accelerated to the desired velocity and then turned back down. This enabled the quantification of how much was lost due to the acceleration and deceleration (if any) of the fan. With this value at hand, it was then possible to quantify the amount lost by subtracting the acceleration losses from the total loss. Again, in anticipation of data

variation, multiple runs were performed in the acceleration phase of the experiment. An average of eight runs was performed. Each of the different velocities had its own set of acceleration phase loss.

The ramping losses values were different for different velocities, with higher losses at higher velocities. This is because all of the acceleration phase experiments were conducted in the same amount of time, approximately 40 seconds, whether the final velocity was 7.2 m/s or 10.3 m/s. For the most part, the acceleration phase losses are one order of magnitude smaller than the overall losses. Although this is not a significant amount because of its magnitude, one has to keep in mind that the some of the overall losses are in the same order of magnitude as the acceleration phase losses. This is the reason why there were approximately eight runs per data point for the graphs presented in Chapter 4. Tables of ramping losses and total amount lost are included in the Appendix.

3.3 Measurement of Velocity

A standard pitot tube was used to measure the velocity. Initially, a hotwire anemometer was proposed in place of the pitot tube due to its ease of use and accuracy. However, due to calibration problems with the instrument, the pitot tube was then preferred over the hotwire anemometer. It was inserted at a height of 15 cm above the tailing sample to measure the velocity in each of the experiments in this study.

As depicted in the schematic of the test stand, there is a mass flow sensor and a flow controller that is mounted onto the ductwork. The mass flow sensor, Kurz Series 155 ADAM, was installed at the location of average velocity after conducting a series of

traverses. This was performed by Gi-Dong Kim, who had previously used the test stand for research. Although the pitot tube was used to determine the velocity in the wind tunnel, the mass flow sensor was used as an initial flow indicator in the duct. After the flow controller was set at the desired flow, the pitot tube was used to measure the velocity. It has to be kept in mind that the mass flow sensor was set at the point of average flow of a circular duct and the pitot tube was set at 15 cm in the center of a rectangle duct with a smaller area. The difference in measurement of the velocities or flows can be seen in the appendix with the pitot tube consistently showing a higher reading than the mass flow sensor, as expected. This would not pose as a problem to the experiment as the velocities mentioned in the experiments were measured by the pitot tube. The flow sensor was used only as an indicator of the velocity in the system.

Chapter 4

RESULTS AND DISCUSSION

The purpose of the experiments was to determine the threshold velocity and entrainment with respect to wind velocity and moisture addition. The laboratory experiment is the simulation of a single possible wind erosion event out in the field. From the tailing samples, the total available erodible material is approximately 13,500 g/m^2, calculated from the average weight of the tailings in the petri dish divided by the area of the petri dish. Theoretically, since there is a finite amount of erodible material available, the erosion process of the tailings from the laboratory experiments is expected to be non-linear. However, the parameters of the experiments were maintained so as not to fully erode all of the available tailings. There were two different sets of experiment that were performed: these were the dry and wet runs for both the threshold velocity and entrainment rate experiments.

In order to determine the threshold velocity, a series of increasing velocity experiments were performed. Five different velocities were chosen to perform the experiment, ranging from 6.9 m/s to 15 m/s. Having chosen the velocities at which the tailings were supposed to be exposed, it was also necessary to determine the desired time of exposure required to get significant entrainment. After a series of trials, it was decided that five minutes of exposure time would suffice.

The threshold velocity was determined using the dry data experiments. Figure 4.1 shows the graph of loss of tailings versus velocity in m/s (measured at a height of 15 cm) for the dry tailings. As shown, it is unclear from the results as to whether the loss rises

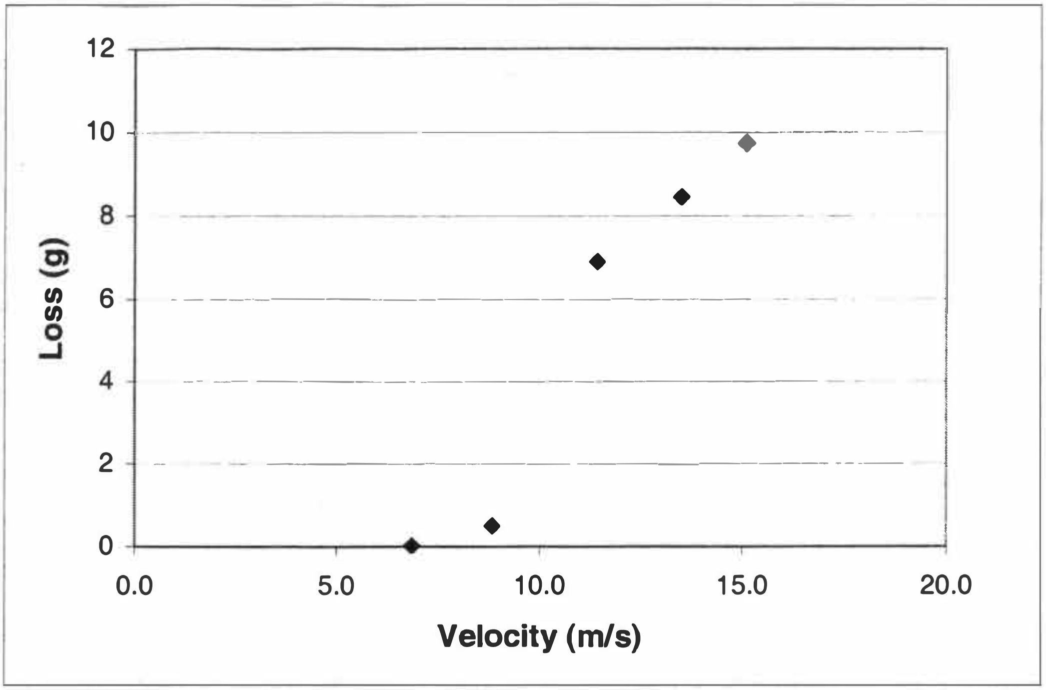

Figure 4.1. Dry Plotted Data

linearly or exponentially, once entrainment is initialized. As such it was uncertain as to whether the data should be fitted to a linear curve or an exponential curve or simply estimated using good judgment. Based on this and other data obtained in the dry and wet tests, it was decided to make a best judgment decision as to the approximate value of the actual threshold velocity. In this study, the approximate threshold velocity was reported as the value at which a loss was first observed. The threshold velocity for the dry data was then determined to be approximately 6.86 m/s, in Figure 4.1.

The same method was used to determine the threshold velocity of the wetted tailings. From Figure 4.2, the threshold velocity was approximated at 8.7 m/s. This value does not appear to show any losses in the graph due to the fact that the losses were minimal, but measurable. Figure 4.3 has a threshold velocity of approximately 11.4 m/s and this data point shows a very minimal loss of tailings. Lastly, the threshold velocity from Figure 4.4 is approximated to be at 14 m/s. There was one more experimental run that was not plotted but is included in the appendix. This experimental run was not plotted because the fan had reached it maximum capacity and yet was not sufficient to cause any entrainment of particles. That value was simply reported as being >15 m/s.

A table summarizing the different threshold velocities is provided in Table 4.1.

Table 4.1. Estimated Threshold Velocities

Moisture added (cm)	0	0.00451	0.0100	0.0143	0.0196
Threshold Velocity (m/s)	6.86	8.70	11.4	14.0	>15

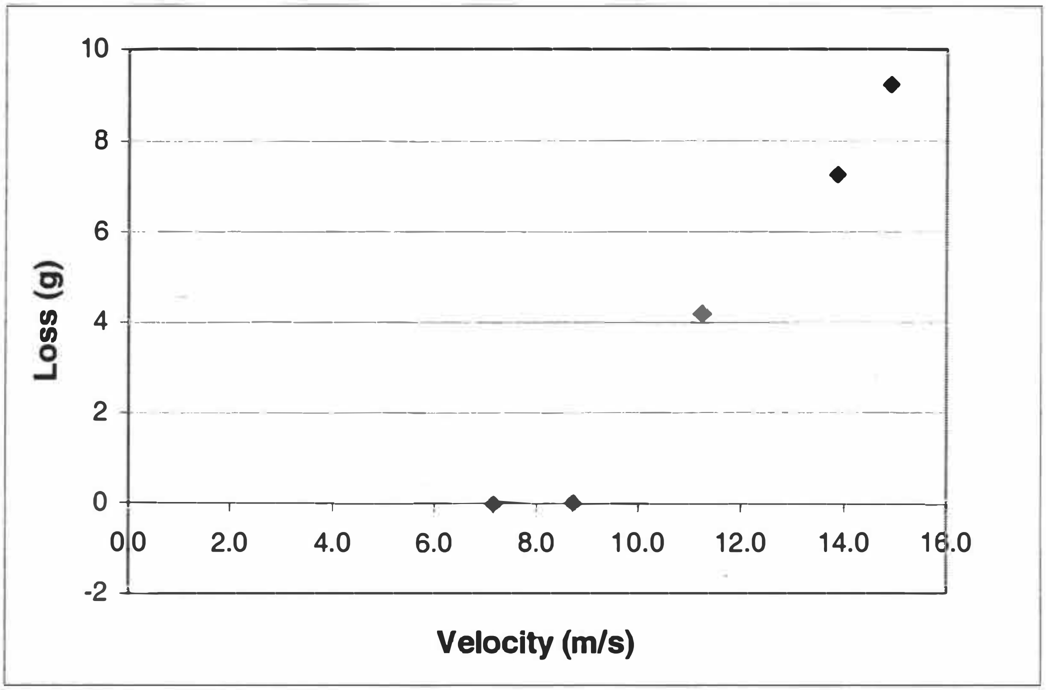

Figure 4.2. Data with 0.00451 cm Water Added

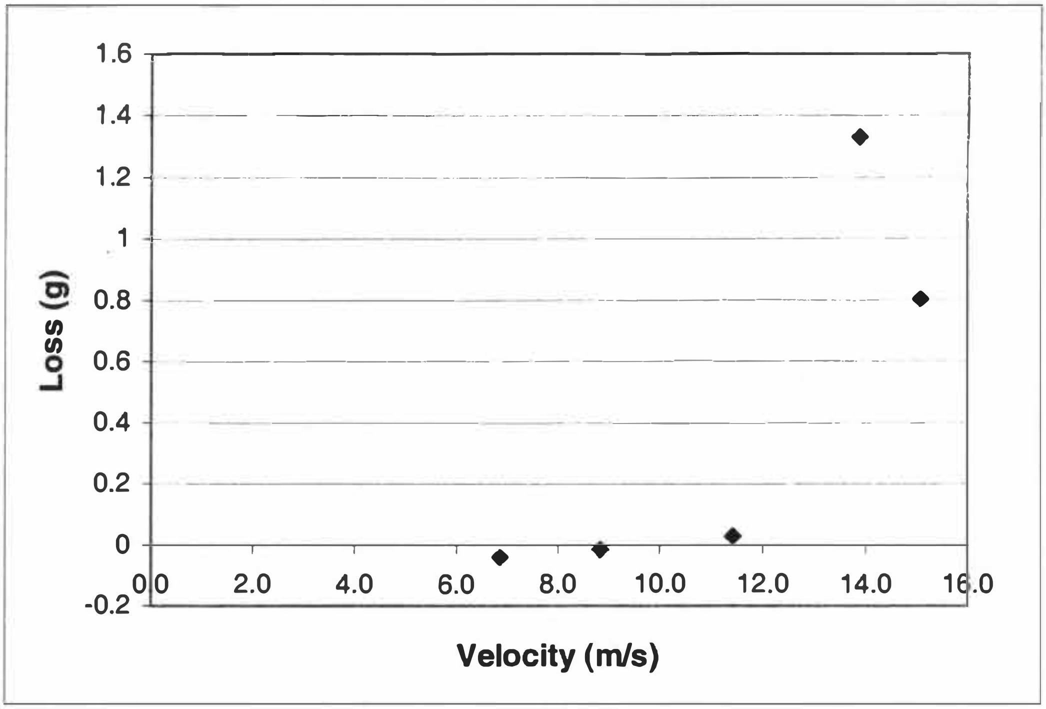

Figure 4.3. Data with 0.01 cm Water Added

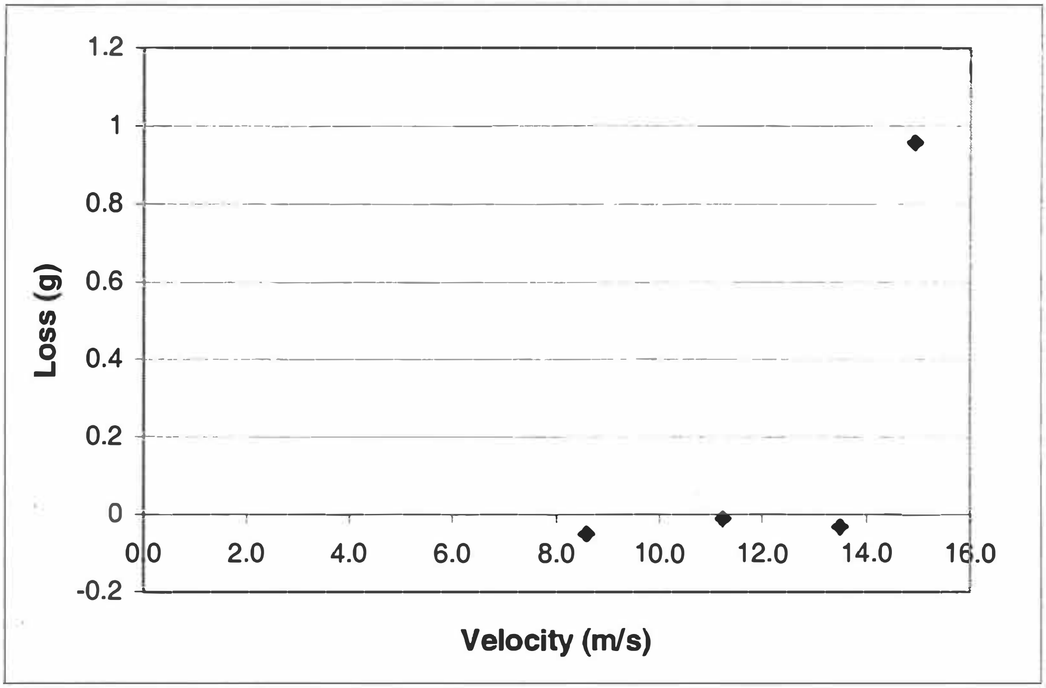

Figure 4.4. Data with 0.0143 cm of Water Added

A graphical description of the relationship between the approximate threshold velocities and different moisture addition is shown in Figure 4.5. The data points on the graph are taken from Table 4.1.

As expected, the more moisture that is added to the sample, the higher the observed threshold velocity. One has to keep in mind that the amount of moisture that is added to the sample for this experiment is extremely low compared to typical rain events that might occur in the real world. The purpose of this experiment was to show how much of an effect moisture could have on the threshold velocity of the tailings. This experiment has demonstrated how sensitive the entrainment of tailings is to the presence of moisture.

This finding is quite important as the site is located geographically where it gets a lot of rainfall in the year, averaging 49.69 inches per year (www.state.tn.us). The minimum amount of measurable rainfall is 0.025 cm (0.01 inches) and this experiment has total moisture levels near the minimum measurable amount of rainfall. Additional discovery was that the tailings were extremely susceptible to humid conditions. This is probably due to the fact that the tailings have 14% or more of particles that are less than 0.072 mm. During an attempt of one experiment in which the laboratory humidity was relatively high, the oven-dried tailings were placed into the petri dish for an extended period. Instead of having the petri dish half empty, it was totally saturated with moisture. In Bagnold's book of Physics of Blown Sand and Desert Dunes, he noticed that particles below the 0.07 mm size had four distinct changes in properties and one of them is that they collect moisture to such an extent they actually bind together and become sticky. AASHTO and ASTM both classify that anything in between the size of 0.05 mm

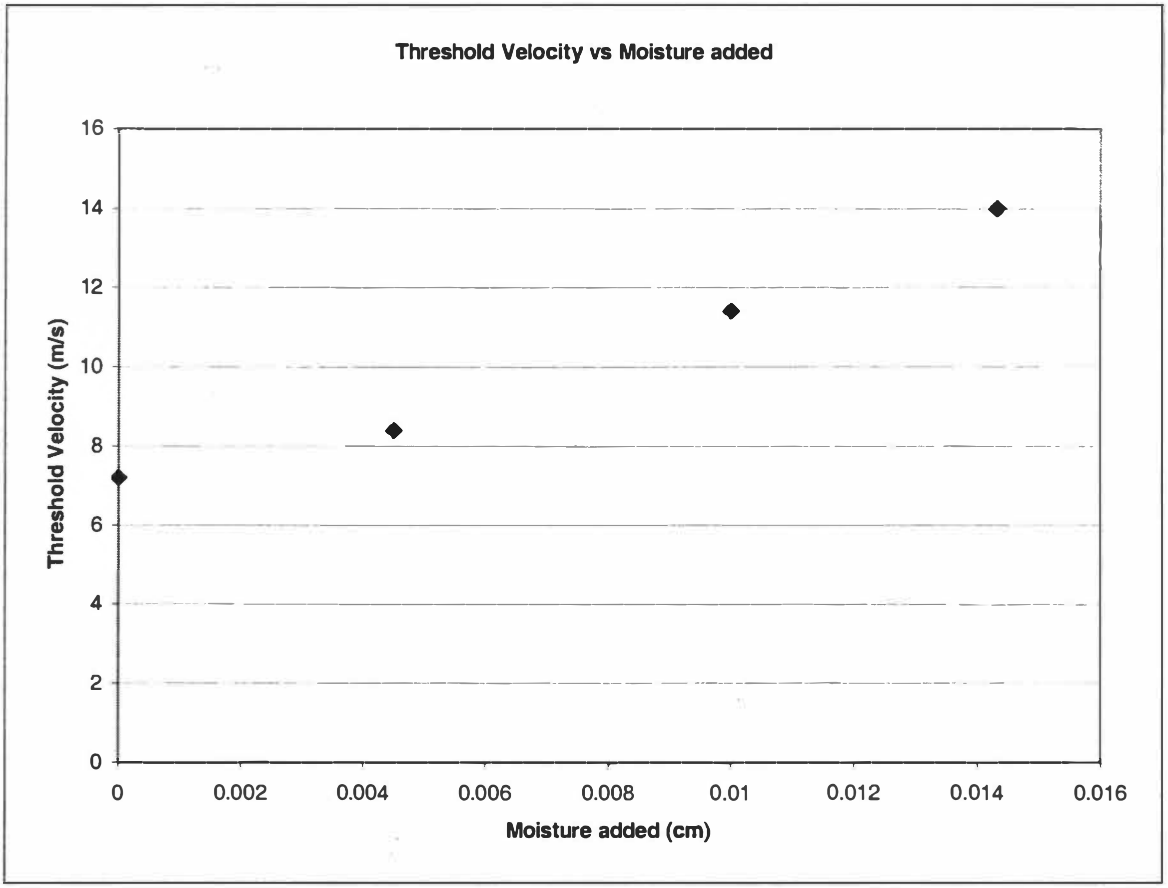

Figure 4.5. Threshold Velocity at Different Moisture Intervals

to 0.002 mm as silt and this makes the particles passing the 200-sieve most probably close to being silt particles.

The other part of this study involved determining the entrainment rate of the tailings. In these tests, the tailings were placed in the petri dish and placed in the wind tunnel. The flow was then ramped up to the desired velocity and maintained at that velocity for specified periods of time ranging up to 45 minutes. The time shown is the time as measured from when the fan was turned on. Approximately 40 seconds elapsed during the acceleration of the fan up to the desired test velocity. Based on the data shown on Figure 4.6, the entrainment rates, in g/min-m^2, were calculated. The slope of each curve was determined by using a least squares fit for the data between 10 and 45 minutes, yielding the entrainment rate in g/min-m^2. At a velocity of 8.4 m/s, the entrainment rate was the highest, at 4.9 g/min-m^2, as compared to the velocity of 7.3 m/s, at 0.4 g/min-m^2. This was expected as higher velocities, should yield greater entrainment rates. However, there is a point that is not included in the graph. This point of interest is the origin (0,0). It is safe to assume that at zero velocity, there would not be any entrainment. The reason why the point is not included in Figure 4.6 is because between the time of zero minute and 10 minutes, the behavior of the dust is not linear. It was not possible to really quantify what happens between zero and 10 minutes. It was later decided that the primary entrainment of interest (i.e. short term reentrainment events as predicted in the AP-42 approach) was primarily concerned with the entrainment that occurred during the first couple of minutes. Thus the entrainment rates associated with the linear curves in Figure 4.6 were of less significance than the initial entrainment that occurred in the first five minutes. This will be discussed further at a later point.

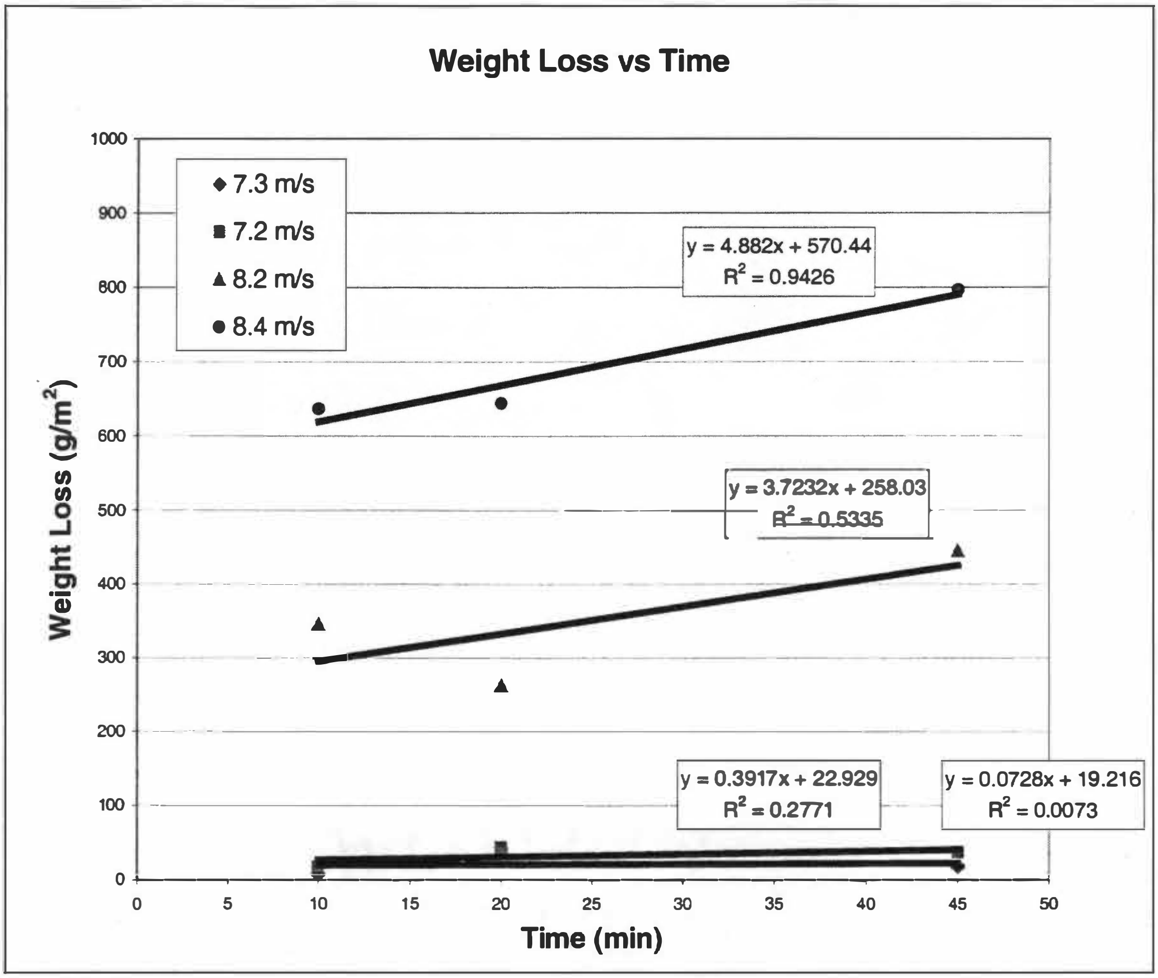

Figure 4.6. Collected Laboratory Dry Data

In the Figure 4.6 there are two low velocity runs. One of them was performed by turning on the fan to produce the desired velocity and the by opening a butterfly valve that exposes the system to the venting system of the building. The latter option of velocity control proved to be a bad choice as results of the experiment did not turn out as well as the one with the control of the fan. This was probably due to the fluctuations of flow in the venting system of the building that caused fluctuations in the reading of the flow meter and weight loss of the sample.

Results of the wet experiments are shown in Figure 4.7 and they display a similar trend of entrainment, although the rates are a lot lower than for the dry experiment. Two vaguely distinct features that can be observed from the graph are the lower entrainment rates and drying phase of the tailings for the 10.3 m/s wind velocity run from the 10 minute to the 20 minute time, causing the big leap between data points. The wetted tailings were essentially a two-phase event, with the first being the evaporation of the moisture added and second being the entrainment phase. Even though the difference in velocities between runs was not that great, the entrainment rates were very different. This was evident from the 10.3 m/s run compared to the 7.2 m/s run. The 7.2 m/s run had virtually zero entrainment, compared to the 10.3 m/s run which had an entrainment rate of 7.82 g/min-m^2. Table 2.1 shows a relationship between particle size and critical velocities with the presence and absence of moisture in the tailings as repeated by Genzel in the literature review. At 7.2 m/s in the present study, there was virtually no entrainment; based on Genzel's data in Table 2.1, this suggests that the particles are larger than 0.25 mm in diameter. Approximately 70% of the tailings were found to be smaller than 0.25 mm from the sieve analysis. It could also be interpreted that the

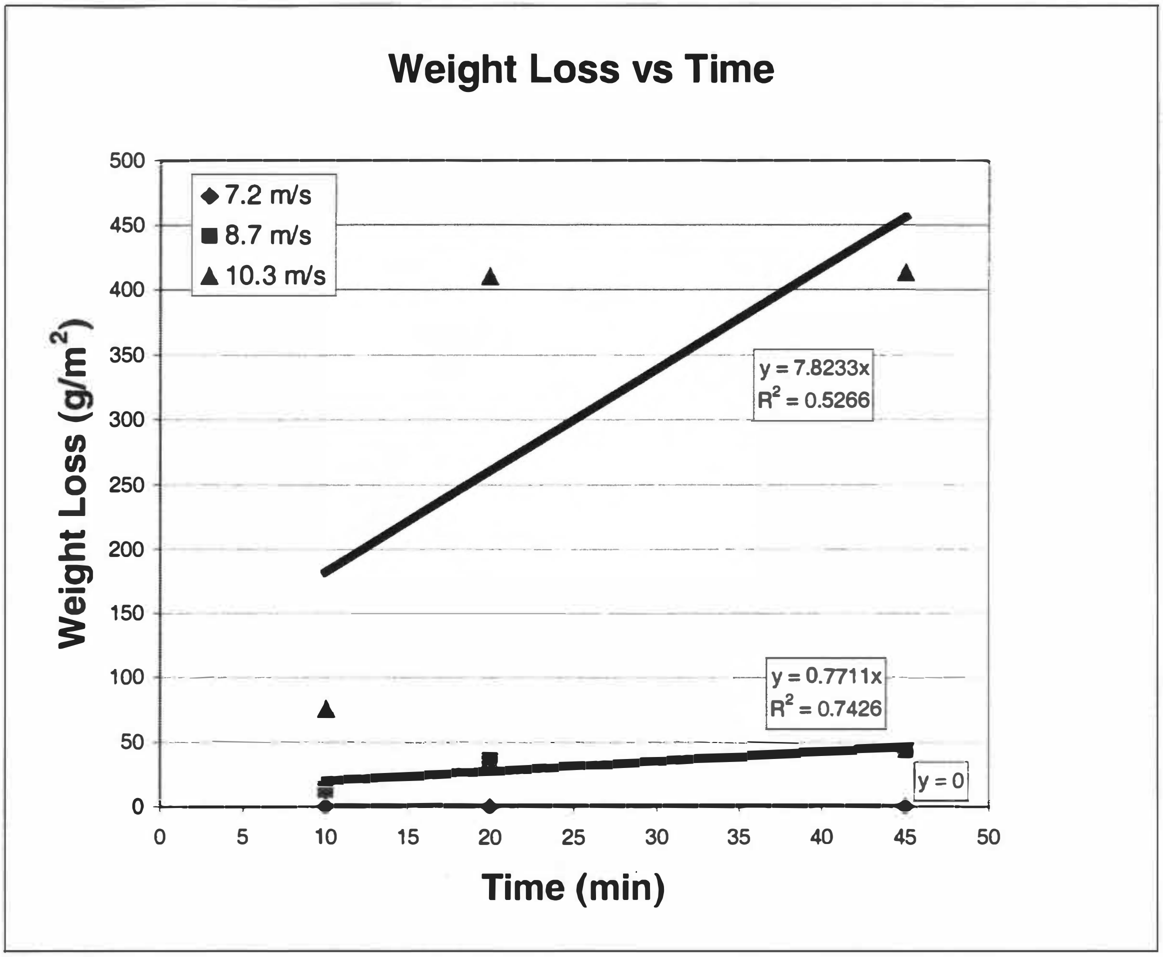

Figure 4.7. Collected Laboratory Wet Data

velocity is too low to overcome the hydrostatic forces of the sample. As there was entrainment at 10.3 m/s, the particle size that was blown off should be between the range 0.25 to 1 mm based on Table 2.1. Then again, it must be kept in mind that the moisture content given in Table 2.1 is 2% and the moisture content equivalent of the sample in this study was only about 0.9%. Conversely, the moisture content at the top portion of the sample could very well be 2% or more because the water was added by means of spraying it over the top of the tailings and not well mixed.

As mentioned before in the previous paragraph, one of the characteristics of the graph was the lower rate of entrainment for the wetted sample. The entrainment rate of the wetted tailings was approximately half that of the dry tailings at the maximum velocity tested for the 45-minute run. Although lower entrainment rates were to be expected from the experiment, it was indeed surprising to find that such a small amount of water added, at about 0.025 cm of water, made such a large difference in the entrainment of the tailings.

One of the reasons was the presence of fine particles that are silt like in the tailings. Due to the fine size of the particles, the presence of even a little water in the tailings made it extremely cohesive thus reducing the entrainment rate greatly. However, when the tailings dries, it crusts up. The crusting nature of the tailings then takes over from the cohesiveness nature of the tailings acting to retard the entrainment of the tailings. It can be seen that there are actually two mechanisms at work here that reduce the entrainment rate of the tailings. This assumption would hold true as long as the surface was not disturbed.

As part of the overall analysis of the laboratory data and the measured erosion values, a comparison was made between the observed data and existing prediction methodology. This prediction methodology was previously mentioned in the literature review as being the AP-42 emissions prediction methodology, Equations 2-3 and 2-4. However, this methodology was designed to predict erosion potential only for dry surfaces and not wet surfaces. With this being the case, only the laboratory dry data results can be compared with the prediction methodology. Hence, the following will be the comparison between the AP-42 prediction methodology and the laboratory dry experimental results, with the latter being discussed first.

Due to the fact that the AP-42 prediction equation calculates the emissions in a particular manner, the dry laboratory data have to be reevaluated differently in order to compare the two. In order to do so, Figure 4.6 will be evaluated in a slightly different manner than before. Figure 4.8 shows the results of the measured erosion from the laboratory experiments in g/m^2, as previously shown in Figure 4.5. The experiments show that the initial erosion or weight loss was quite large, after which it reduced to a smaller amount with time. The data in Figure 4.8 for the 10, 20 and 45 minutes tests were extrapolated linearly back to time t = 0 minutes. This was done in order to estimate the erosion that would have occurred that would be attributed to the short-term single erosion event. As shown in the figure, these values were approximately 258 g/m^2 and 570 g/m^2 for the 8.2 m/s and 8.4 m/s velocities, respectively. These values represent the actual erosion potential for the total loss, which occurred in the laboratory test, not the erosion potential as calculated in the AP-42 emission prediction methodology for less than certain aerodynamic particle sizes. Thus it was necessary to determine the percent of the tailings

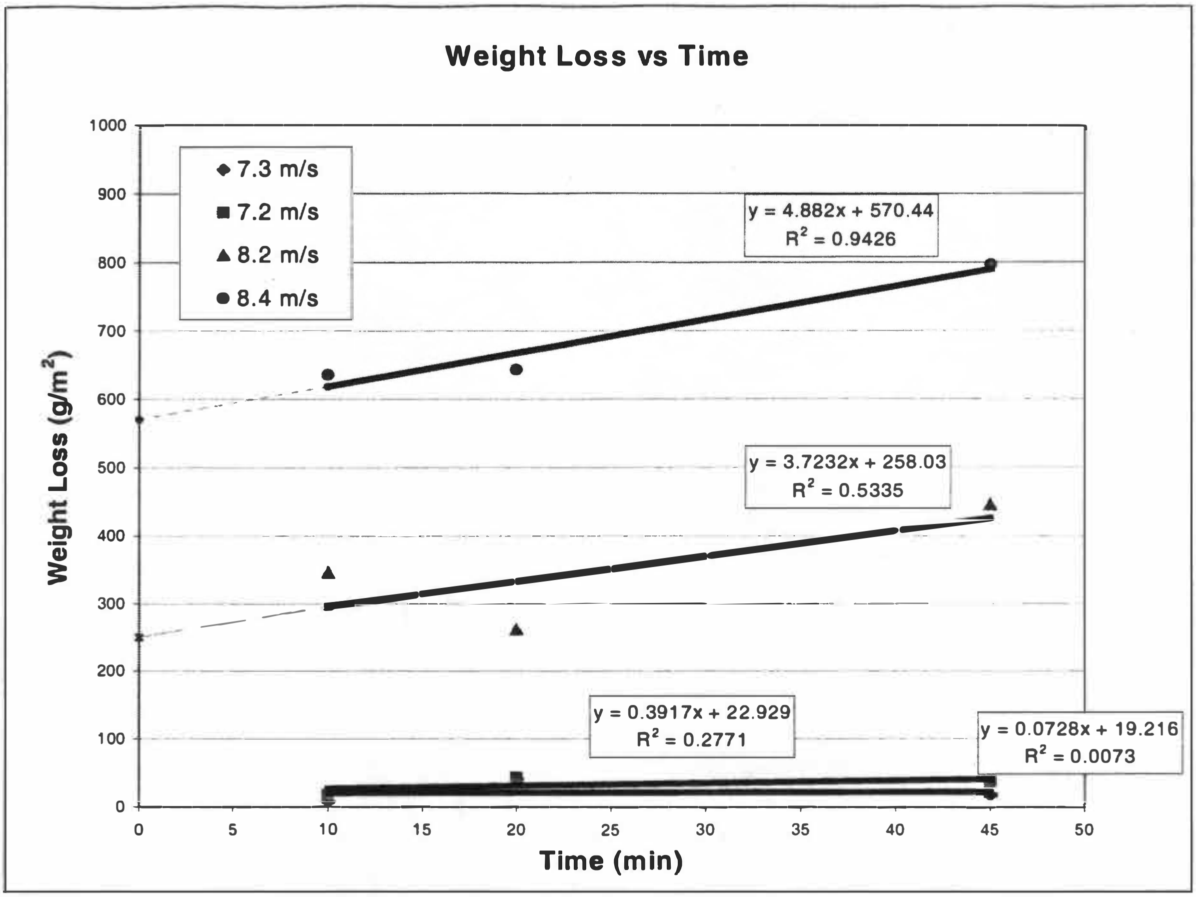

Figure 4.8. Collected Laboratory Dry Data with Extrapolation

that were less than 30, 15, 10 and 2.5 μm aerodynamic particle size in order to compare the erosion potential with that predicted by AP-42. A particle size analysis was conducted on the tailings using the following procedure. First, the tailings were sieved through a 200-mesh sieve to determine the percentage that passed this mesh size. It was found to be 12.48%. A sample of the tailings passing the 200-mesh sieve was then sent to Micromeretics Laboratory to determine its particle size distribution (i.e. the fraction less 30, 15, 10 and 2.5 μm aerodynamic particle size).

The particle size analysis conducted by Micromeretics Laboratory was performed using a sedigraph analyze, which determines the percentage of particles less than or equal to stated size by mass. The stated size is the diameter of the equivalent spherical particle based on sedimentation that has the same density as the particle in question. The particle density, as measured and reported by Micromeretics Laboratory, was 3.36 g/cm^3 and is actually input into the instrument to be used as part of the analysis. Thus the particle size as reported by Micromeretics Laboratory is not the 'aerodynamic' particle size, rather the size based on a density of 3.36 g/cm^3. In an effort to correct this to the equivalent spherical size of the particle with unit density, it was necessary to further correct this size using the equation:

$$d_{aero} = d_{sedigraph} \times (\rho_p)^{0.5} \qquad (4.1)$$

For example, if the sedigraph stated that 50% of the particles were less than particle size of 10 μm with a density of 3.36 g/cm^3, then this is equivalent to stating that 50% of the particle mass lies below an aerodynamic particle size of 10*(3.36)^0.5 or 18.3 μm aerodynamic size. Or restated, if one wants to know the percent of particles (based on aerodynamic particle size) less than 10 μm, then one would actually look up the

percentage less than or equal to a 10/(3.36)^0.5 or 5.45 µm particle with density of 3.36 g/cm^3 which is what is plotted on the Sedigraph output. The particle size distribution is shown in Figure 4.9 for the results of the sedigraph analysis. Based on the distribution, the percentage less than 10 µm aerodynamic size is 6.4%. Using the same analytical approach, the Sedigraph particle sizes representing 30, 15, 10 and 2.5 µm aerodynamic diameters are 16.36, 8.18, 5.45 and 1.36 µm respectively. Therefore, the percentages less than 30, 15, 10 and 2.5 µm are 20%, 9.1%, 6.4% and 2.6%.

Based on the above discussion, if a total of 570 g/m^2 of weight loss occurred, and assuming that this occurred for all particle sizes in the laboratory wind tunnel, then the actual quantity of erosion for particles less than 30 µm aerodynamic size would be 570 g/m^2 times the percentage of particles less than 30 µm aerodynamic size. The percentage is only 20% of the 12.48% which was sent to Micromeretics Laboratory. Thus, the erosion potential was 570 g/m^2 * 0.1248 * 0.2 or 14.23 g/m^2. Similarly, the weight loss for the particles less than 15, 10 and 2.5 µm aerodynamic diameters were 6.47 g/m^2, 4.55 g/m^2 and 1.85 g/m^2. Table 4.2 is a summary of the laboratory results.

Table 4.2. Results of Laboratory Experiments

Velocity	8.2 m/s	8.4 m/s
Diameter	Weight loss g/m^2	
30 µm	6.440	14.23
15 µm	2.930	6.473
10 µm	2.061	4.553
2.5 µm	0.837	1.850

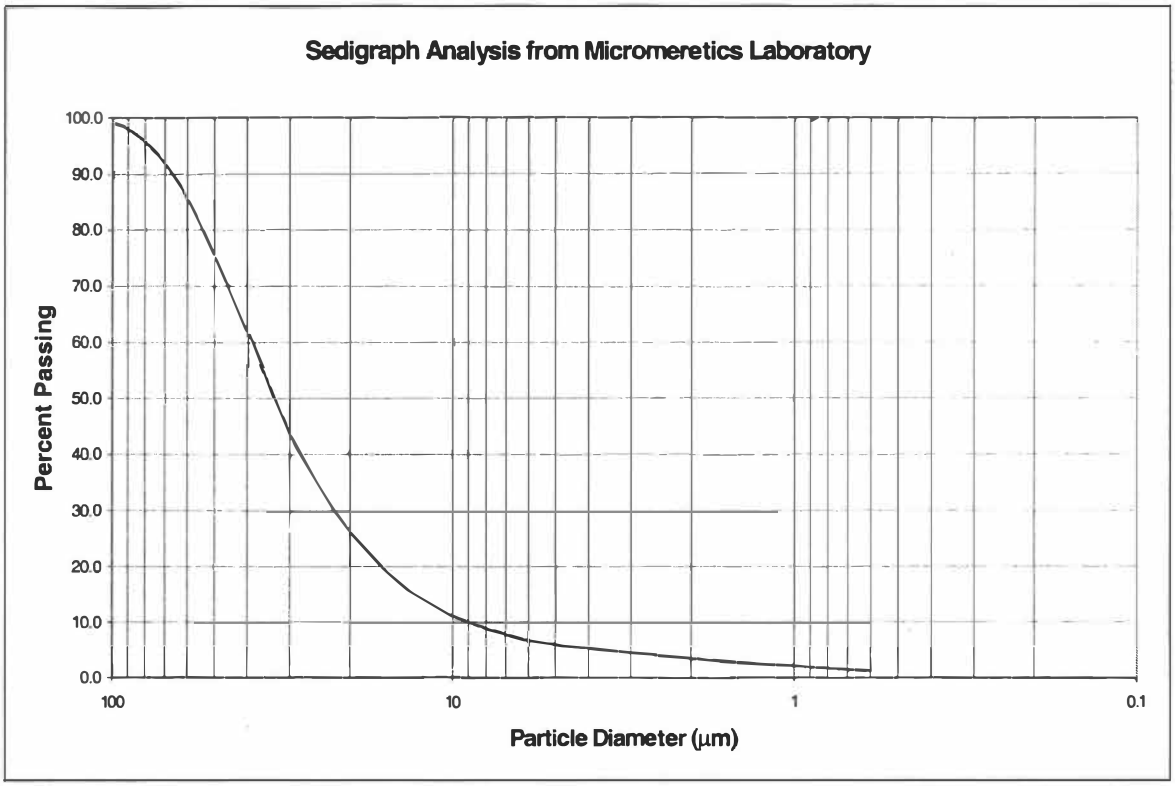

Figure 4.9. Micromeretics Laboratory particle analysis (sedigraph analysis) chart.

In the document Compilation of Air Pollution Emissions Factors AP-42, prediction methodologies are provided for estimation of emissions for a variety of sources. However, only one of the prediction methodologies is of interest in this particular discussion. The prediction methodology of interest is provided in AP-42 Chapter 13, section 13.2.5, titled Industrial Wind Erosion. Equation 2.3 in the literature review estimates the potential amount of dust emissions that can be generated by wind erosion of open aggregate storage piles in an industrial facility. The potential erosion equation is extremely susceptible to changes in friction velocities associated with the material of concern because it is a function of both the threshold friction velocity and friction velocity as shown in Equation 2.4. Total erosion potential calculated from this equation can be made for a single erosion event or for an entire year. Only the single erosion event will be considered in this case since the laboratory experiments were performed to simulate single erosion events, not an entire year.

A multiplier is used in the calculation of the erosion potential, *k*, as shown in Equation 2.3, to provide a calculation of the erosion potential for particles less than or equal to four specific aerodynamic particle sizes, 30 μm, 15 μm, 10 μm and 2.5 μm. This multiplier is particle size sensitive and there are four different values that are provided by the AP-42 document, less than 30 μm, less than 15 μm, less than 10 μm and less than 2.5 μm with *k* values of 1.0, 0.6, 0.5 and 0.2 respectively. These multipliers are used to determine the different amount of particulate matter (PM) pollution with respect to particle size, for regulation purposes. Again, the AP-42 equations were developed only for dry exposed surfaces.

Another equation that was presented in the AP-42 document is the calculation of the friction velocity and threshold friction velocity, u^* and u_t^*. These are important parameters for the calculation of the erosion potential as the equation is expressed as a function of both the friction velocity and the threshold friction velocity. In addition the velocity at any height z is related to the friction velocity measured at the roughness height z_o as follows:

$$u(z) = \frac{u^*}{0.4} \ln \frac{z}{z_o} \qquad (z > z_o) \qquad (4.2)$$

The equation is an expression of the wind speed profile in the surface boundary layer, whereby the wind above the surface follows a logarithmic velocity profile as it extends above the surface. The z term in the equation is the height at which the velocity was measured and z_o is the roughness height. Roughness height is a measurement of roughness of an exposed surface (i.e. the average size of an object obstruction), usually in terms of length (i.e. cm, m, ft, etc). With this in mind, one can see that roughness height is not a constant. Although, there are tables and charts that provide roughness height values, they are usually approximations of what is actually in the environment. This being the case, it was decided that a range of roughness heights would be used in order to get an idea of the range of the erosion potential that can be generated from the AP-42 equation. This would help in determining the approximate roughness height of the tailings. The u^* term in the equation is a measure of the wind shear stress on the erodible surface and $u(z)$ is the velocity which is measured at height z.

In all of the laboratory experiments, the wind velocities were measured at a height of 15 cm above the surface of the tailings. From Equation 4.2, two of the four variable

terms could be measured, i.e. wind velocity, *u(z)* and height at which velocity was measured, *z*. The third term, z_o, as mentioned before, is just an approximation and a range of z_o's were used. With these data, u^* could then be calculated by rearranging Equation 4.2. For example, if the measured velocity, at 15 cm, is 8.2 m/s and z_o is estimated to be 0.5 cm, then u^* would be 8.2*0.4/ln (15/0.5). This calculation is repeated throughout a set of analyses with a range of different z_o's (ranging from 0.01 cm to 0.5 cm) and two different velocities, 8.2 m/s and 8.4 m/s. A table summarizing the calculation of the erosion potential with different z_o's and velocities is provided in Table 4.3. The threshold friction velocity could also be determined by using Equation 4.2. One would start with rearranging the equation so that the friction velocity term, u^*, is expressed as a function of the measured velocity, *u(z)*, and the natural logarithm of *z* over z_o. Consequently, if the threshold velocity of the tailings was to be substituted as the velocity measured, which was 6.86 m/s, the resulting threshold friction velocity would be (6.86*0.4)/ln (15/0.5), at a z_o of 0.5 cm, or 0.81 m/s. For assumed roughness heights of 0.01 to 0.5 cm, the threshold friction velocity is estimated to range from 0.37 to 0.81 m/s.

Results from the laboratory experiments consistently showed higher erosion potential than the calculated values as can be seen in Table 4.2 and Table 4.3, respectively. Plausible explanations for this occurrence will be addressed.

Table 4.3. AP-42 Potential Erosion Estimation at Different z_o's and Velocities

Velocity	8.2 m/s @ z = 15 cm				8.4 m/s @ z = 15 cm			
z_o (cm)	0.5	0.3	0.03	0.01	0.5	0.3	0.03	0.01
Diameter	Weight Loss g/m^2							
30 µm	5.3802	3.3380	2.5877	2.1439	6.4355	3.9501	3.0479	2.5173
15 µm	3.2281	2.0028	1.5526	1.2863	3.8613	2.3700	1.8287	1.5104
10 µm	2.6901	1.6690	1.2938	1.0719	3.2178	1.9750	1.5239	1.2586
2.5 µm	1.0760	0.6676	0.5175	0.4288	1.2871	0.7900	0.6096	0.50346

Although the difference of velocity between 8.2 m/s and 8.4 m/s is only marginal, the erosion potential for the laboratory results showed a significantly different picture. The erosion potential at 8.2 m/s is about half of that of the 8.4 m/s. The 8.2 m/s laboratory data compared reasonably well with calculated values at a z_o of 0.5 cm. However, for the more reasonable values of roughness height (between 0.03 to 0.3 cm), the measured values were higher than predicted by approximately a factor of two. On the other hand, for the 8.4 m/s data collected from the laboratory experiments yielded data that were a factor of two to three times higher than the prediction methodology.

There are a several possible reasons for the differences between the calculated and laboratory results. First of all, the setup of the laboratory system did not allow for short timed duration runs. The typical time measurements were 10 minutes, 20 minutes and 45 minutes. However, all these data points plotted out a straight lined graph that could be extrapolated to where time was zero. This was done because AP-42 calculations were stated as being erosion events of short-term duration (approximately 1 to 2 minutes).

Another possible reason why the laboratory results were higher than the theoretical data may have been due to the fact that the laboratory tailings were oven dried, which meant that they had no moisture in them. This condition would allow for higher erosion potential because there is no moisture present to bind the particles together. When the AP-42 equations and factors were developed, the experiments were performed onsite, where the coal storage piles were not completely dry. Further laboratory experiments showed that the tailings were extremely sensitive to the presence of moisture. In addition to the presence of moisture, the laboratory tailings were completely disturbed samples. The AP-42 equation that was developed used undisturbed

samples that were onsite. Tailings that were used in the laboratory experiments were procured from a composite of locations to ensure that a representative sample was obtained. The size of the average particles that were present in the tailings was small, typically less than 0.02 cm in diameter, thus forming a conducive situation for a higher potential of erosion.

In the above discussion, the threshold friction velocity was determined based on the observed threshold velocity at 15 cm for a range of assumed surface roughness, z_o, and varied from 0.37 to 0.81 m/s. It is worthwhile to note that AP-42 (Table 13.2.5-2) also provides recommended threshold friction velocities for a number of different materials, as shown in Table 4.4. It is notable that the range of threshold friction velocities for several of the materials (i.e. scraper tracks, fine coal dust, ground coal) are similar in value to those calculated in this study. It is also possible to calculate the threshold friction velocity using Gillette's equation for disturbed soils, given in the literature review as Equation 2.7. The *Mode* that was used in the equation is 190 μm based on the size distribution of the tailings as presented in Figure 3.1. Based on this technique, the threshold friction velocity would have been 0.45 m/s, again within the range of the values determined in this study. Based on this value, one can now also calculate a corresponding roughness height, z_o, using Equation 4.2 of 0.03 cm. The values obtained in this study for copper tailings are included in the table for comparison. An additional column of data was added to the AP-42 table, threshold velocity at 15 cm, as a comparison of available threshold velocities if they were measured at 15 cm above the sample, as in the case of the laboratory experiments.

Table 4.4. Threshold Friction Velocity Comparison Between AP-42 Data and Laboratory Results

Material	Threshold Friction Velocity (m/s)	Roughness Height (cm)	Threshold Velocity at 10 m (m/s) z_o = act	Threshold Velocity at 15 cm (m/s) z_o = act
Overburden	1.02	0.3	21	10.0
Scoria (roadbed material)	1.33	0.3	27	13.0
Ground Coal (surrounding coal pile)	0.55	0.01	16	10.1
Uncrusted coal pile	1.12	0.3	23	11.0
Scraper tracks on coal pile	0.62	0.06	15	8.6
Fine coal dust on concrete pad	0.54	0.2	11	5.8
Copper tailings*	0.45	0.03	12	6.86

*determined from this study

AP-42 also provides a table (Table 13.2.5-1) which allows the user to determine the threshold friction velocity based on the use of Tyler sieves. Figure 4.10 shows the graph of the AP-42 predicted threshold friction velocities as a function of the mean particle size reportedly taken from a 1952 laboratory procedure published by W.S. Chepil. In an effort to further investigate the relationship between friction velocity and particle size, Gillette's equation for both disturbed and undisturbed soils in Equations 2.7 and 2.8 were also used. Both equations provide a linear graph as compared to the non-linear graph that AP-42 presents (see Figure 4.10). The other method that was used was Bagnold's equation for static friction velocity, as provided in the literature review as Equation 2-2. The equation provided a non-linear graph, similar looking in curvature to the one of AP-42. In spite of this, Bagnold's results plotted somewhat lower than that of the AP-42 numbers. All of these can be seen in Figure 4.10. It is noted that none of the graphs were identical to the one provided in AP-42. Further, as stated earlier, while these values are in the same general range as the those found in this study, the use of these values in the AP-42 erosion potential equation resulted in predicted erosion potential that was two to four times the values measured in this study.

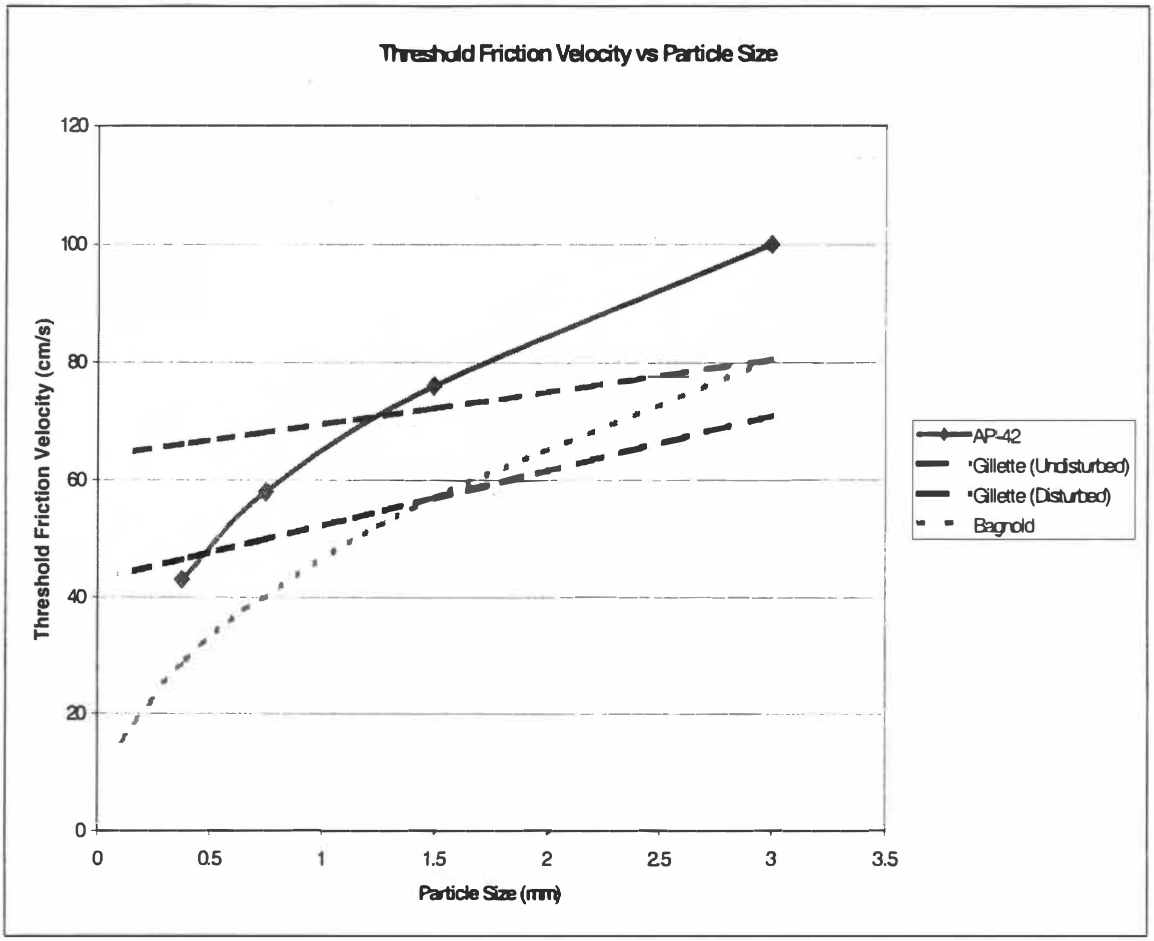

Figure 4.10. Threshold Friction Velocity as a Function of Particle Size

Chapter 5

CONCLUSION AND RECOMMENDATIONS

Among all of the findings, one of the most interesting was how the tailings reacted to the amount of water that was added to it. The threshold velocity of the dry tailings doubled from 6.86 m/s (with zero moisture) to 14 m/s with only 0.0143 cm of water addition. This amount of water addition is not even within the measurable rainfall as reported by the NWS, which is 0.025 cm (0.01 inch). This increase in velocity was probably due to the presence of fine particles that would make the tailings cohesive even with very little amounts of water.

The other part of the laboratory experiments involves the determination of the entrainment rates of the tailings. Two sets of entrainment potential experiments were performed, dry and wet. However, only the dry set of experiments could be used for comparison with an existing prediction methodology as the prediction methodology was developed only for dry surfaces. The laboratory results consistently showed higher entrainment values than the prediction methodology. As mentioned previously, one of the possible reasons for this was that the tailings were completely dried, without any moisture to hold the particles together. On the other hand, the AP-42 prediction equation was developed by performing the experiments onsite, which meant that samples used were not completely dried. As demonstrated in both the threshold velocity and wetted entrainment potential experiments, slight amounts of moisture were sufficient to greatly increase the threshold velocity and reduce the entrainment potential. Another possible reason for the higher values was due to the fact that the laboratory experiments were

carried out with disturbed tailings. The AP-42 prediction methodology was developed onsite for undisturbed soils.

Recommendation for improvements lie in the area of better design of ductwork, better control of ambient conditions (i.e. temperature and humidity) and setting up a particle capture device so that particle analysis could be done. One particular improvement that could potentially help better determine weight loss is setting up the wind tunnel so that the tailings would not be exposed to the ramping losses of the fan and would just be exposed to the desired velocity of wind speed directly. This could enable better quantification of the behavior of the tailings between zero and ten minutes.

Areas for future research could include studying the evaporation characteristics and how these affects the entrainment rates and understand what different levels of humidity have on the effect of entrainment rates. One particular experiment that could yield interesting results would be sieving out the portion of the tailings that passes the 200-mesh sieve (0.072 mm sieve opening) and performing similar tests on the tailings without this portion and also performing similar tests on the portion that passed the 200-sieve alone.

Bibliography

Bibliography

AP-42, Compilation of Air Pollution Emissions Factors, Chapter 13: Miscellaneous Sources (1/95), 13.2.5 Industrial wind erosion

Bagnold, R.A., 1941 *The Physics of Blown Sand and Desert Dunes*, Methuen, London.

Cernica, J.N., 1995 *Soil Mechanics*, John Wiley & Sons Inc, New York.

Chepil, W.S., Properties of soil which influence wind erosion IV, State of dry aggregate structure, *Soil Science*, 72, 387 – 401, 1951.

Chow, Judith C. (1997), Measurement Methods to Determine Compliance with Ambient Air Quality Standards for Suspended Particles, *Journal of the Air and Waste Management Association,* Vol. 47, September,1002-1003.

Fuchs, N.A., 1964 *The Mechanics of Aerosols*, Pergamon Press, London.

Gillette, D.A., 1980 "Threshold Velocities for Input of Soil Particles Into the air by Desert Soils", *Journal of Geophysical Research,* 85 (C10): 5621-5630

http://www.qub.ac.uk/geosci/teaching/postgrad/workshop1/erosion4.html, 7/12/00

http://www.state.tn.us/education/webfacts.htm

Micromeretics Laboratory, Analysis of tailings for particle size distribution and particle density, Norcross GA, January 5, 2001

Price, J.C., Vasher, D.R., Vitton, S.J., Paterson, K.G. 1998 "Characterization of fugitive dust emissions from the tailings of a Northern Michigan iron mine", *Journal of Tailings and Mine Waste,* Balkema, Rotterdam.

Wind Erosion on European Light Soils (WEELS), "Technical Report to the European Union Commission for the period: 1/2/99 to 31/12/99", http://www.geog.ucl.ac.uk/weels/

Appendix

Entrainment Rate Experiment Raw Data (dry)

450 (w/o fan) cfm data

10 Minute Run

Wt before	Wt after	Difference	Static Press("wg)	ΔP("wg)	Kurz meter (cfm)	$\Delta P^{1/2}$("wg)	Velocity (fps)
23.4637	23.4487	0.015	0.9	0.12	430	0.346	23.46
23.5582	23.5577	0.0005	0.85	0.14	440	0.374	25.32
23.9834	23.9788	0.0046	0.875	0.125	440	0.354	23.93
24.1617	24.152	0.0097	0.85	0.14	445	0.374	25.32
24.0448	24.0215	0.0233	0.85	0.12	445	0.346	23.44

	Wt before	Wt after	Difference	Static Press	ΔP	Kurz		Velocity
Ave =	23.8424	23.8317	0.0106	0.8650	0.1290	440		24.29
σ =	0.3110	0.3090	0.0089					0.9555

20 minute Run*

Wt before	Wt after	Difference	Static Press("wg)	ΔP("wg)	Kurz meter (cfm)	$\Delta P^{1/2}$("wg)	Velocity (fps)
23.1204	23.0476	0.0728	0.9	0.14	445	0.374	25.34
23.3875	23.35	0.0375	0.85	0.12	430	0.346	23.44
23.1406	23.0936	0.047	0.85	0.13	430	0.361	24.40

	Wt before	Wt after	Difference	Static Press	ΔP	Kurz		Velocity
Ave =	23.2162	23.1637	0.0524	0.8667	0.1300	435		24.39
σ =	0.1487	0.1629	0.0183					0.9501

* Only had three runs because the results were similar to the 10 min runs.

45 minute Run

Wt before	Wt after	Difference	Static Press("wg)	ΔP("wg)	Kurz meter (cfm)	$\Delta P^{1/2}$("wg)	Velocity (fps)
23.4677	23.4477	0.02	0.85	0.12	430	0.346	23.44
22.9974	23.0138	-0.0164	0.9	0.12	435	0.346	23.46
23.0132	22.9645	0.0487	0.9	0.12	430	0.346	23.46
22.8509	22.8517	-0.0008	0.85	0.12	430	0.346	23.44
23.0562	22.978	0.0782	0.85	0.12	420	0.346	23.44
23.3487	23.3323	0.0164	0.86	0.11	420	0.332	22.45

	Wt before	Wt after	Difference	Static Press	ΔP	Kurz		Velocity
Ave =	23.1224	23.0980	0.0243	0.8533	0.1167	423		23.11
σ =	0.2502	0.2492	0.0415					0.4093

450 cfm data

Ramping losses

Wt before	Wt after	Difference
23.0736	23.0623	0.0113
23.3589	23.3483	0.0106
23.1673	23.1696	-0.0023
23.4431	23.4309	0.0122
23.4977	23.4954	0.0023
24.4035	24.3956	0.0079
23.7208	23.7215	-0.0007
24.1982	24.211	-0.0128
23.42	23.4108	0.0092

Average = 0.004189
Std Dev = 0.008314

10 Minute Run

Wt before	Wt after	Difference	Static Press("wg)	ΔP("wg)	Kurz meter (cfm)	$\Delta P^{1/2}$("wg)	Velocity (fps)
23.4	23.38	0.02	1	0.125	450	0.354	23.99
22.542	22.4573	0.0847	1.05	0.115	450	0.339	23.03
23.1818	23.1781	0.0037	1.05	0.12	454	0.346	23.52
22.8037	22.7989	0.0048	1.05	0.125	453	0.354	24.01
24.2993	24.2741	0.0252	1.05	0.12	450	0.346	23.52
23.5415	23.5158	0.0257	1.05	0.12	452	0.346	23.52
22.9057	22.8577	0.048	1.05	0.12	451	0.346	23.52
22.471	22.4533	0.0177	1.05	0.125	455	0.354	24.01
Ave = 23.1431	23.1144	0.0287	1.0438	0.1213	452		23.64
σ = 0.6033	0.6112	0.0265					0.3425

20 minute Run

Wt before	Wt after	Difference	Static Press("wg)	ΔP("wg)	Kurz meter (cfm)	$\Delta P^{1/2}$("wg)	Velocity (fps)
23.3751	23.3349	0.0402	1.05	0.12	453	0.346	23.52
24.4428	24.36	0.0828	1	0.12	450	0.346	23.50
24.4529	24.35	0.1029	1.05	0.12	453	0.346	23.52
23.5465	23.5179	0.0286	1.05	0.125	452	0.354	24.01
23.8182	23.6615	0.1567	1.05	0.125	452	0.354	24.01
23.1638	23.1295	0.0343	1.05	0.125	450	0.354	24.01
23.3354	23.31	0.0254	1.05	0.12	451	0.346	23.52
23.1144	23.0693	0.0451	1.05	0.115	447	0.339	23.03
Ave = 23.6561	23.5916	0.0645	1.0438	0.1213	451		23.64
σ = 0.5358	0.5081	0.0463					0.3467

45 minute Run

Wt before	Wt after	Difference	Static Press("wg)	ΔP("wg)	Kurz meter (cfm)	$\Delta P^{1/2}$("wg)	Velocity (fps)
23.0327	22.9683	0.0644	1.05	0.125	451	0.354	24.01
22.3984	22.4244	-0.026	1	0.12	448	0.346	23.50
23.4237	23.3349	0.0888	1.05	0.125	454	0.354	24.01
23.6429	23.5506	0.0923	1.05	0.12	450	0.346	23.52
22.6627	22.5906	0.0721	1	0.12	452	0.346	23.50
23.0269	22.9867	0.0402	1	0.125	449	0.354	23.99

Ave =	23.0312	22.9759	0.0553	1.0250	0.1225	451		23.76
σ =	0.4614	0.4271	0.0440					0.2696

500 cfm data

Ramping losses

Wt before	Wt after	Difference
23.0838	23.0685	0.0153
23.71	23.6835	0.0265
24.1072	24.0184	0.0888
23.3553	23.2749	0.0804
23.68	23.626	0.054
23.8417	23.7545	0.0872
23.5586	23.5359	0.0227
23.9726	23.9354	0.0372
23.67	23.6054	0.0646

Average = 0.0530 g
Std Dev = 0.0288 g

10 Minute Run

	Wt before	Wt after	Difference	Static Press("wg)	ΔP("wg)	Kurz meter (cfm)	$\Delta P^{1/2}$("wg)	Velocity (fps)
	23.2939	22.8642	0.4297	1.2	0.155	500	0.394	26.80
	23.523	22.7476	0.7754	1.25	0.16	500	0.400	27.26
	23.4843	22.8405	0.6438	1.25	0.15	500	0.387	26.39
	23.8344	23.3473	0.4871	1.2	0.155	500	0.394	26.80
	23.508	23.0668	0.4412	1.25	0.16	500	0.400	27.26
	22.8157	22.6588	0.1569	1.15	0.155	490	0.394	26.78
	21.9355	21.0305	0.905	1.2	0.16	510	0.400	27.23
	23.5357	23.1227	0.413	1.2	0.155	490	0.394	26.80
Ave =	23.2413	22.7098	0.5315	1.2125	0.1563	499		26.92
σ =	0.6020	0.7141	0.2350					0.3080

20 minute Run

	Wt before	Wt after	Difference	Static Press("wg)	ΔP("wg)	Kurz meter (cfm)	$\Delta P^{1/2}$("wg)	Velocity (fps)
	22.7308	22.2621	0.4687	1.2	0.16	495	0.400	27.23
	22.507	21.7886	0.7184	1.2	0.16	505	0.400	27.23
	23.4735	23.1524	0.3211	1.2	0.155	500	0.394	26.80
	23.9	23.5391	0.3609	1.2	0.165	500	0.406	27.66
	23.7736	23.5625	0.2111	1.2	0.16	500	0.400	27.23
Ave =	23.2770	22.8609	0.4160	1.2000	0.1600	500		27.23
σ =	0.6254	0.7977	0.1925					0.3009

45 minute Run

Wt before	Wt after	Difference	Static Press("wg)	ΔP("wg)	Kurz meter (cfm)	$\Delta P^{1/2}$("wg)	Velocity (fps)
23.8875	22.0889	1.7986	1.2	0.16	501	0.400	27.23
23.9023	23.2231	0.6792	1.2	0.16	504	0.400	27.23
24.6974	24.355	0.3424	1.15	0.15	497	0.387	26.35
23.6024	22.7895	0.8129	1.2	0.16	505	0.400	27.23
23.5447	22.6521	0.8926	1.15	0.16	496	0.400	27.21
23.1203	22.6541	0.4662	1.2	0.16	504	0.400	27.23
22.7845	22.6541	0.1304	1.15	0.16	505	0.400	27.21
22.4561	22.2166	0.2395	1.2	0.16	500	0.400	27.23
Ave = 23.4994	22.8292	0.6702	1.1813	0.1588	502		27.12
σ = 0.7075	0.7072	0.5304					0.3117

525 cfm data

Ramping losses

Wt before	Wt after	Difference
23.6235	23.4053	0.2182
23.4743	23.4112	0.0631
24.08	23.8816	0.1984
23.0918	22.7717	0.3201
23.5966	23.49	0.1066
23.8156	23.6845	0.1311
23.27	23.1117	0.1583
23.1487	23.03	0.1187

Average = 0.164313 g
Std Dev = 0.080294 g

10 Minute Run

	Wt before	Wt after	Difference	Static Press("wg)	ΔP("wg)	Kurz meter (cfm)	$\Delta P^{1/2}$("wg)	Velocity (fps)
	22.8238	22.1971	0.6267	1.3	0.165	520	0.406	27.70
	22.7857	21.604	1.1817	1.3	0.16	524	0.400	27.28
	24.0663	23.4268	0.6395	1.3	0.16	520	0.400	27.28
	23.1484	22.3234	0.825	1.3	0.17	523	0.412	28.12
	23.85	23.0334	0.8166	1.3	0.16	528	0.400	27.28
	24.3764	23.7121	0.6643	1.3	0.17	530	0.412	28.12
	23.8307	21.7355	2.0952	1.3	0.17	524	0.412	28.12
	23.6495	22.13	1.5195	1.3	0.17	520	0.412	28.12
Ave =	23.5664	22.5203	1.0461	1.3000	0.1656	524		27.75
σ =	0.5854	0.7798	0.5253					0.4160

20 minute Run

	Wt before	Wt after	Difference	Static Press("wg)	ΔP("wg)	Kurz meter (cfm)	$\Delta P^{1/2}$("wg)	Velocity (fps)
	24.3113	22.1911	2.1202	1.3	0.165	528	0.406	27.70
	23.2112	22.36	0.8512	1.25	0.16	527	0.400	27.26
	23.2072	21.83	1.3772	1.3	0.17	531	0.412	28.12
	23.7412	23.1424	0.5988	1.3	0.17	525	0.412	28.12
	22.4749	20.8638	1.6111	1.3	0.16	523	0.400	27.28
	23.184	22.874	0.31	1.3	0.165	520	0.406	27.70
	22.9112	21.5314	1.3798	1.3	0.16	524	0.400	27.28
	22.9112	21.5314	1.3798	1.3	0.165	530	0.406	27.70
Ave =	23.0445	21.9886	1.0559	1.3000	0.1640	524		27.62
σ =	0.4650	0.9745	0.5664					0.3516

45 minute
Run

Wt before	Wt after	Difference	Static Press("wg)	ΔP("wg)	Kurz meter (cfm)	$\Delta P^{1/2}$("wg)	Velocity (fps)
23.1517	22.2965	0.8552	1.3	0.165	529	0.406	27.70
22.8308	21.8668	0.964	1.3	0.17	525	0.412	28.12
23.5351	21.8638	1.6713	1.3	0.17	524	0.412	28.12
23.9946	22.412	1.5826	1.3	0.165	529	0.406	27.70

Ave =	23.3781	22.1098	1.2683	1.3000	0.1675	527		27.91
σ =	0.5018	0.2862	0.4181					0.2405

Entrainment Rate Experiment Raw Data (wet)

450 cfm data with moisture

Ramping losses

Dish #	Dry weight	Wet weight	Weight after run	Moisture gain	Moisture loss	Weight loss
7	23.3426	23.3938	23.3564	0.0512	0.0374	-0.0138
10	22.8865	23.0063	22.9563	0.1198	0.05	-0.0698
11	23.16	23.3957	23.3331	0.2357	0.0626	-0.1731
12	23.2991	23.4382	23.3818	0.1391	0.0564	-0.0827
13	23.6721	23.7247	23.6515	0.0526	0.0732	0.0206
14	22.5224	22.6008	22.5549	0.0784	0.0459	-0.0325
15	22.71	22.8452	22.7787	0.1352	0.0665	-0.0687
			Average =	0.1160	0.0560	
			Mean =	0.1016	0.0548	

Average moisture left in sample is = 0.0600g

10 min Run

Dish #	Initial dry weight (g)	Initial wet weight (g)	Wet weight after run (g)	Moisture added (g)	Weight loss (g)	Dry basis wt loss (g)	Static Press("wg)	ΔP("wg)	Kurz meter (cfm)	$\Delta P^{1/2}$("wg)	Velocity (fps)
16	23.6878	23.8057	23.6863	0.1179	0.1194	0.0015	1.05	0.12	455	0.346	23.52
17	22.4886	22.6474	22.5076	0.1588	0.1398	-0.019	1.05	0.115	454	0.339	23.03
18	22.88	23.0218	22.8983	0.1418	0.1235	-0.0183	1.05	0.12	450	0.346	23.52
19	23.4451	23.5927	23.4516	0.1476	0.1411	-0.0065	1.05	0.12	453	0.346	23.52
20	22.8775	22.944	22.8683	0.0665	0.0757	0.0092	1.05	0.12	453	0.346	23.52
1	22.804	22.9862	22.8476	0.1822	0.1386	-0.0436	1.05	0.12	449	0.346	23.52
2	23.3466	23.487	23.3665	0.1404	0.1205	-0.0199	1.05	0.115	451	0.339	23.03
3	23.02	23.3716	23.11	0.3516	0.2616	-0.09	1.05	0.12	450	0.346	23.52
Average =	23.0687	23.2321	23.0920	0.1634	0.1400	-0.0233					23.40
Std Dev =	0.3934	0.3915	0.3867	0.0832	0.0535	0.0313					

20 min Run

Dish #	Initial dry weight (g)	Initial wet weight (g)	Wet weight after run (g)	Moisture added (g)	Weight loss (g)	Dry basis wt loss (g)	Static Press("wg)	ΔP("wg)	Kurz meter (cfm)	$\Delta P^{1/2}$("wg)	Velocity (fps)
4	22.8371	23.1334	22.85	0.2963	0.2834	-0.0129	1	0.12	448	0.346	23.50
5	22.9879	23.1635	22.9955	0.1756	0.168	-0.0076	1	0.12	454	0.346	23.50
7	23.0439	23.1459	23.0478	0.102	0.0981	-0.0039	1.05	0.12	447	0.346	23.52
8	23.24	23.3742	23.2436	0.1342	0.1306	-0.0036	1	0.12	450	0.346	23.50
9	22.384	22.5247	23.3826	0.1407	-0.8579	-0.9986	1	0.125	456	0.354	23.99
10	22.89	23.19	22.9386	0.3	0.2514	-0.0486	1	0.12	451	0.346	23.50
11	22.6473	22.7752	22.6454	0.1279	0.1298	0.0019	1	0.12	451	0.346	23.50
12	23.2634	23.402	23.2617	0.1386	0.1403	0.0017	1	0.12	452	0.346	23.50
Average =	22.9117	23.0886	23.0457	0.1769	0.0430	-0.1340				Average =	23.57
Std Dev =	0.2950	0.2969	0.2426	0.0775	0.3696	0.3498					

45 min Run

Dish #	Initial dry weight (g)	Initial wet weight (g)	Wet weight after run (g)	Moisture added (g)	Weight loss (g)	Dry basis wt loss (g)	Static Press("wg)	ΔP("wg)	Kurz meter (cfm)	$\Delta P^{1/2}$("wg)	Velocity (fps)
13	23.8751	23.9854	23.8756	0.1103	0.1098	-0.0005	1.05	0.125	450	0.354	24.01
14	22.7203	22.8535	22.7243	0.1332	0.1292	-0.004	1.05	0.12	448	0.346	23.52
15	23.2332	23.4168	23.242	0.1836	0.1748	-0.0088	1	0.12	449	0.346	23.50
16	22.8846	23.074	22.8868	0.1894	0.1872	-0.0022	1.05	0.12	451	0.346	23.52
17	22.6777	22.8548	22.684	0.1771	0.1708	-0.0063	1.05	0.115	453	0.339	23.03
18	23.0136	23.0653	23.0056	0.0517	0.0597	0.008	1.05	0.12	444	0.346	23.52
19	22.5467	22.7252	22.54	0.1785	0.1852	0.0067	1.05	0.125	450	0.354	24.01
20	23.6451	23.835	23.644	0.1899	0.191	0.0011	1	0.12	451	0.346	23.50
Average =	23.0745	23.2263	23.0753	0.1517	0.1510	-0.0007				Average =	23.58
Std Dev =	0.4770	0.4721	0.4773	0.0497	0.0471	0.0059					

Moisture Added = 0.025cm rainfall

Percent Moisture = 1.0%

550 cfm data with moisture

Ramping losses

Dish #	Dry weight	Wet weight	Weight after run	Moisture gain	Moisture loss	Weight loss
1	21.6624	21.7644	21.7022	0.102	0.0622	-0.0398
2	22.5829	22.7347	22.674	0.1518	0.0607	-0.0911
3	22.4691	22.6418	22.5807	0.1727	0.0611	-0.1116
4	22.1842	22.3246	22.2706	0.1404	0.054	-0.0864
5	23.8442	24.02	23.9581	0.1758	0.0619	-0.1139
7	23.9237	24.2065	24.1421	0.2828	0.0644	-0.2184
8	23.5486	23.81	23.7548	0.2614	0.0552	-0.2062
9	22.6337	22.78	22.7215	0.1463	0.0585	-0.0878
			Average =	0.1791	0.0597	
			Mean =	0.1705	0.0597	

Average moisture left in sample is = 0.1194g

10 min Run

Dish #	Initial dry weight (g)	Initial wet weight (g)	Wet weight after run (g)	Moisture added (g)	Weight loss (g)	Dry basis wt loss (g)	Static Press("wg)	ΔP("wg)	Kurz meter (cfm)	$\Delta P^{1/2}$("wg)	Velocity (fps)
10	23.0366	23.1944	23.0562	0.1578	0.1382	-0.0196	1.55	0.17	552	0.412	28.25
11	22.8881	22.96	22.72	0.0719	0.24	0.1681	1.55	0.165	550	0.406	27.83
12	23.1161	23.2356	23.1036	0.1195	0.132	0.0125	1.55	0.175	556	0.418	28.66
13	23.6292	23.7421	23.6182	0.1129	0.1239	0.011	1.55	0.17	548	0.412	28.25
15	24.2921	24.3878	24.2764	0.0957	0.1114	0.0157	1.55	0.17	548	0.412	28.25
16	23.4159	23.5752	23.4263	0.1593	0.1489	-0.0104	1.55	0.17	550	0.412	28.25
17	23.3	23.4028	23.3744	0.1028	0.0284	-0.0744	1.5	0.17	561	0.412	28.22
19	23.8861	23.9781	23.8465	0.092	0.1316	0.0396	1.5	0.17	548	0.412	28.22
Average =	23.4455	23.5595	23.4277	0.1140	0.1318	0.0178	1.538	0.17	551.63		28.24
Std Dev =	0.4710	0.4655	0.4897	0.0310	0.0576	0.0695					

20 min Run

Dish #	Initial dry weight (g)	Initial wet weight (g)	Wet weight after run (g)	Moisture added (g)	Weight loss (g)	Dry basis wt loss (g)	Static Press("wg)	ΔP("wg)	Kurz meter (cfm)	$\Delta P^{1/2}$("wg)	Velocity (fps)
1	22.6345	22.7528	22.63	0.1183	0.1228	0.0045	1.5	0.17	550	0.412	28.22
2	22.5278	22.617	22.4952	0.0892	0.1218	0.0326	1.5	0.175	550	0.418	28.63
3	22.632	22.7724	22.6075	0.1404	0.1649	0.0245	1.55	0.17	556	0.412	28.25
4	22.7947	22.8889	22.757	0.0942	0.1319	0.0377	1.5	0.17	548	0.412	28.22
5	24.1275	24.2205	24.0364	0.093	0.1841	0.0911	1.5	0.17	551	0.412	28.22
7	23.6792	23.8138	23.6031	0.1346	0.2107	0.0761	1.5	0.17	548	0.412	28.22
8	23.3438	23.4616	23.3132	0.1178	0.1484	0.0306	1.5	0.165	551	0.406	27.80
9	22.37	22.48	22.2649	0.11	0.2151	0.1051	1.55	0.17	556	0.412	28.25
Average =	23.0137	23.1259	22.9634	0.1122	0.1625	0.0503	1.513	0.17	551.25		28.23
Std Dev =	0.6302	0.6303	0.6176	0.0192	0.0377	0.0358					

45 min Run

Dish #	Initial dry weight (g)	Initial wet weight (g)	Wet weight after run (g)	Moisture added (g)	Weight loss (g)	Dry basis wt loss (g)	Static Press("wg)	ΔP("wg)	Kurz meter (cfm)	$\Delta P^{1/2}$("wg)	Velocity (fps)
10	22.0379	22.1909	21.9482	0.153	0.2427	0.0897	1.5	0.18	553	0.424	29.04
11	22.3947	22.52	22.3773	0.1253	0.1427	0.0174	1.5	0.175	554	0.418	28.63
12	23.4277	23.5749	23.3979	0.1472	0.177	0.0298	1.5	0.18	546	0.424	29.04
13	23.0616	23.1524	22.9244	0.0908	0.228	0.1372	1.5	0.18	549	0.424	29.04
14	22.5285	22.6374	22.4068	0.1089	0.2306	0.1217	1.5	0.175	550	0.418	28.63
15	23.05	23.16	22.9966	0.11	0.1634	0.0534	1.5	0.18	556	0.424	29.04
16	22.9986	23.12	22.98	0.1214	0.14	0.0186	1.5	0.175	548	0.418	28.63
19	23.3035	23.3825	23.2862	0.079	0.0963	0.0173	1.5	0.17	554	0.412	28.22
Average =	22.8503	22.9673	22.7897	0.1170	0.1776	0.0606	1.500	0.18	551.25		28.79
Std Dev =	0.4805	0.4703	0.4983	0.0255	0.0521	0.0492					

Moisture
Added = 0.023cm rainfall
Percent Moisture = 0.8%

650 cfm data with moisture

Ramping losses

Dish #	Dry weight	Wet weight	Weight after run	Moisture gain	Moisture loss	Weight loss
20	23.1009	23.2439	23.1751	0.143	0.0688	-0.0742
1	22.67	22.8008	22.74	0.1308	0.0608	-0.07
2	22.2221	22.4341	22.3725	0.212	0.0616	-0.1504
3	22.5571	22.7129	22.6557	0.1558	0.0572	-0.0986
4	22.7784	23.0611	23.0059	0.2827	0.0552	-0.2275
5	23.9833	24.1535	24.0949	0.1702	0.0586	-0.1116
7	24.2525	24.41	24.3478	0.1575	0.0622	-0.0953
8	23.39	23.4826	23.4279	0.0926	0.0547	-0.0379
			Average =	0.1681	0.0599	
			Mean =	0.1602	0.0597	

Average moisture left in sample is = 0.1082g

10 min Run

Dish #	Initial dry weight (g)	Initial wet weight (g)	Wet weight after run (g)	Moisture added (g)	Weight loss (g)	Dry basis wt loss (g)	Static Press("wg)	ΔP("wg)	Kurz meter (cfm)	$\Delta P^{1/2}$("wg)	Velocity (fps)
10	22.3383	22.47	22.2964	0.1317	0.1736	0.0419	2	0.24	657	0.490	33.84
11	23.09	23.2109	22.8847	0.1209	0.3262	0.2053	2	0.24	654	0.490	33.84
12	23.054	23.3418	23.122	0.2878	0.2198	-0.068	2	0.24	663	0.490	33.84
13	24	24.1413	23.7486	0.1413	0.3927	0.2514	2	0.24	652	0.490	33.84
15	23.6511	23.8157	23.67	0.1646	0.1457	-0.0189	2	0.235	648	0.485	33.48
16	23.0416	23.1512	22.9418	0.1096	0.2094	0.0998	2	0.24	648	0.490	33.84
17	22.975	23.1513	22.9748	0.1763	0.1765	0.0002	2	0.24	649	0.490	33.84
19	22.8167	22.9216	22.4976	0.1049	0.424	0.3191	2	0.235	665	0.485	33.48
Average =	23.1208	23.2755	23.0170	0.1546	0.2585	0.1039	2.000	0.24	654.50		33.75
Std Dev =	0.5060	0.5148	0.5052	0.0593	0.1073	0.1402					

20 min Run

Dish #	Initial dry weight (g)	Initial wet weight (g)	Wet weight after run (g)	Moisture added (g)	Weight loss (g)	Dry basis wt loss (g)	Static Press("wg)	ΔP("wg)	Kurz meter (cfm)	$\Delta P^{1/2}$("wg)	Velocity (fps)
17	21.9718	22.0543	21.68	0.0825	0.3743	0.2918	2	0.24	661	0.490	33.84
18	22.4996	22.64	22.2723	0.1404	0.3677	0.2273	2	0.24	650	0.490	33.84
19	23.1917	23.2621	22.7896	0.0704	0.4725	0.4021	2	0.23	651	0.480	33.12
20	23.4648	23.5507	22.4528	0.0859	1.0979	1.012	2	0.24	655	0.490	33.84
1	23.2949	23.4322	23.2164	0.1373	0.2158	0.0785	2	0.235	648	0.485	33.48
2	22.0862	22.1148	21.8444	0.0286	0.2704	0.2418	2	0.24	661	0.490	33.84
3	22.7808	22.9059	22.2858	0.1251	0.6201	0.495	2	0.24	654	0.490	33.84
4	22.9316	23.0272	22.1356	0.0956	0.8916	0.796	2	0.24	650	0.490	33.84
Average =	22.7777	22.8734	22.3346	0.0957	0.5388	0.4431	2.000	0.2	653.75		33.70
Std Dev =	0.5529	0.5667	0.4947	0.0378	0.3119	0.3152					

45 min Run

Dish #	Initial dry weight (g)	Initial wet weight (g)	Wet weight after run (g)	Moisture added (g)	Weight loss (g)	Dry basis wt loss (g)	Static Press("wg)	ΔP("wg)	Kurz meter (cfm)	$\Delta P^{1/2}$("wg)	Velocity (fps)
5	22.7745	22.8838	22.5415	0.1093	0.3423	0.233	2	0.24	656	0.490	33.84
7	23.2423	23.3547	23.1648	0.1124	0.1899	0.0775	2	0.235	666	0.485	33.48
8	23.1135	23.2315	22.7776	0.118	0.4539	0.3359	2	0.24	661	0.490	33.84
9	22.7004	22.8239	22.4027	0.1235	0.4212	0.2977	2	0.24	646	0.490	33.84
10	22.38	22.5141	21.5746	0.1341	0.9395	0.8054	2	0.235	654	0.485	33.48
11	21.88	22.0142	20.0414	0.1342	1.9728	1.8386	2	0.24	658	0.490	33.84
2	22.5711	22.7127	22.165	0.1416	0.5477	0.4061	2	0.245	648	0.495	34.19
5	22.7822	22.8841	22.2	0.1019	0.6841	0.5822	2	0.24	661	0.490	33.84
Average =	22.6805	22.8024	22.1085	0.1219	0.6939	0.5721	2.0	0.239	656.25		33.79
Std Dev =	0.4252	0.4167	0.9567	0.0139	0.5640	0.5576					

Moisture Added = 0.023cm rainfall

Percent Moisture = 0.9%

Threshold Velocity Determination Raw Data (5 minute runs)

450 cfm

Dish #	Initial dry weight (g)	Initial wet weight (g)	Wet weight after run (g)	Moisture added (g)	Weight loss (g)	Dry basis wt loss (g)	Static Press("wg)	ΔP("wg)	Kurz meter (cfm)	$\Delta P^{1/2}$("wg)	Velocity (fps)	Velocity (m/s)
8	22.7742	0	22.7556	0	0.0186	0.0186	1.05	0.11	450	0.332	22.52	6.86
9	22.3334	22.4153	22.3521	0.0819	0.0632	-0.0187	1	0.12	450	0.346	23.50	7.16
10	22.3	22.425	22.3408	0.125	0.0842	-0.0408	1	0.11	450	0.332	22.50	6.86
Average =	22.4692	14.9468	22.4828	0.0690	0.0553	-0.0136	1.017	0.1	450.00		22.84	6.96
Std Dev =	0.2647	12.9443	0.2363	0.0635	0.0335	0.0300						0.17

550 cfm

Dish #	Initial dry weight (g)	Initial wet weight (g)	Wet weight after run (g)	Moisture added (g)	Weight loss (g)	Dry basis wt loss (g)	Static Press("wg)	ΔP("wg)	Kurz meter (cfm)	$\Delta P^{1/2}$("wg)	Velocity (fps)	Velocity (m/s)
13	23.169	0	22.6751	0	0.4939	0.4939	1.4	0.18	550	0.424	28.99	8.84
14	21.9943	22.0921	21.9868	0.0978	0.1053	0.0075	1.5	0.175	545	0.418	28.63	8.73
15	22.8362	22.9423	22.8512	0.1061	0.0911	-0.015	1.4	0.18	551	0.424	28.99	8.84
16	22.8872	23.0379	22.9379	0.1507	0.1	-0.0507	1.4	0.17	554	0.412	28.17	8.59
17	22.2522	22.51	22.41	0.2578	0.1	-0.1578	1.5	0.17	554	0.412	28.22	8.60
18	22.66	22.8911	22.79	0.2311	0.1011	-0.13	1.4	0.18	539	0.424	28.99	8.84
Average =	22.6332	18.9122	22.6085	0.1406	0.1652	0.0247	1.433	0.2	548.83		28.67	8.74
Std Dev =	0.4352	9.2717	0.3552	0.0947	0.1611	0.2387						0.12

750 cfm

Dish #	Initial dry weight (g)	Initial wet weight (g)	Wet weight after run (g)	Moisture added (g)	Weight loss (g)	Dry basis wt loss (g)	Static Press("wg)	ΔP("wg)	Kurz meter (cfm)	$\Delta P^{1/2}$("wg)	Velocity (fps)	Velocity (m/s)
19	22.8247	0	15.9193	0	6.9054	6.9054	2.4	0.29	750	0.539	37.47	11.42
3	22.7353	22.7766	18.5566	0.0413	4.22	4.1787	2.5	0.28	739	0.529	36.88	11.24
4	22.86	22.9921	22.8312	0.1321	0.1609	0.0288	2.4	0.29	752	0.539	37.47	11.42
5	22.882	23.038	22.8922	0.156	0.1458	-0.0102	2.5	0.28	754	0.529	36.88	11.24
7	23.4206	23.692	23.5624	0.2714	0.1296	-0.1418	2.4	0.29	745	0.539	37.47	11.42
8	23.2338	23.54	23.3847	0.3062	0.1553	-0.1509	2.4	0.29	748	0.539	37.47	11.42
Average =	22.9927	19.3398	21.1911	0.1512	1.9528	1.8017	2.433	0.3	748.00		37.27	11.36
Std Dev =	0.2704	9.4809	3.1859	0.1215	2.9223	3.0237						0.09

900 cfm

Dish #	Initial dry weight (g)	Initial wet weight (g)	Wet weight after run (g)	Moisture added (g)	Weight loss (g)	Dry basis wt loss (g)	Static Press("wg)	ΔP("wg)	Kurz meter (cfm)	$\Delta P^{1/2}$("wg)	Velocity (fps)	Velocity (m/s)
9	22.0439	0	13.5909	0	8.453	8.453	3.4	0.39	889	0.624	44.27	13.49
10	22.0507	22.0918	14.7924	0.0411	7.2994	7.2583	3.5	0.41	907	0.640	45.48	13.86
11	22.2947	22.4575	20.9645	0.1628	1.493	1.3302	3.5	0.41	894	0.640	45.48	13.86
3	23.2668	23.5329	23.2979	0.2661	0.235	-0.0311	3.4	0.39	905	0.624	44.27	13.49
4	23.0808	23.3055	23.1332	0.2247	0.1723	-0.0524	3.4	0.39	907	0.624	44.27	13.49
5	23.3258	23.627	23.4426	0.3012	0.1844	-0.1168	3.4	0.39	905	0.624	44.27	13.49
Average =	22.6771	19.1691	19.8703	0.1660	2.9729	2.8069	3.433	0.4	901.17		44.68	13.62
Std Dev =	0.6117	9.4110	4.5071	0.1224	3.8485	3.9662						0.19

1000 cfm

Dish #	Initial dry weight (g)	Initial wet weight (g)	Wet weight after run (g)	Moisture added (g)	Weight loss (g)	Dry basis wt loss (g)	Static Press("wg)	ΔP("wg)	Kurz meter (cfm)	$\Delta P^{1/2}$("wg)	Velocity (fps)	Velocity (m/s)
18	22.4791	0	12.7236	0	9.7555	9.7555	3.8	0.48	978	0.693	49.50	15.09
16	22.75	22.8004	13.5158	0.0504	9.2846	9.2342	3.7	0.47	985	0.686	48.89	14.90
19	22.8631	23.0286	22.06	0.1655	0.9686	0.8031	3.7	0.48	1004	0.693	49.40	15.06
7	23.0569	23.2753	22.0993	0.2184	1.176	0.9576	3.8	0.47	1014	0.686	48.98	14.93
8	23.2376	23.5687	23.4008	0.3311	0.1679	-0.1632	3.7	0.49	1015	0.700	49.91	15.21
9	22.5557	22.834	22.6429	0.2783	0.1911	-0.0872	3.7	0.48	978	0.693	49.40	15.06
Average =	22.8237	19.2512	19.4071	0.1740	3.5906	3.4167	3.733	0.5	995.67		49.35	15.04
Std Dev =	0.2909	9.4355	4.9007	0.1290	4.6131	4.7328						0.11

AP-42 Predicted Erosion Potential

8.2 m/s velocity (at 15 cm above surface)

z_o = 0.5 cm

u^*_t = 0.80677 m/s (with 6.86 m/s being the threshold velocity)

u^* = 0.96437 m/s (8.2 m/s)

	u^*	u^*_t	P
30 µm	0.96437	0.80677	5.38022
15 µm	0.96437	0.80677	3.22813
10 µm	0.96437	0.80677	2.69011
2.5 µm	0.96437	0.80677	1.07604

z_o = 0.1 cm

u^*_t = 0.54764 m/s (with 6.86 m/s being the threshold velocity)

u^* = 0.65461 m/s (8.2 m/s)

	u^*	u^*_t	P
30 µm	0.65461	0.54764	3.33801
15 µm	0.65461	0.54764	2.00281
10 µm	0.65461	0.54764	1.66901
2.5 µm	0.65461	0.54764	0.66760

z_o = 0.03 cm

u^*_t = 0.44154 m/s (with 6.86 m/s being the threshold velocity)

u^* = 0.52779 m/s (8.2 m/s)

	u^*	u^*_t	P
30 µm	0.52779	0.44154	2.58766
15 µm	0.52779	0.44154	1.55260
10 µm	0.52779	0.44154	1.29383
2.5 µm	0.52779	0.44154	0.51753

z_o = 0.01 cm

u^*_t = 0.37521 m/s (with 6.86 m/s being the threshold velocity)

u^* = 0.44850 m/s (8.2 m/s)

	u^*	u^*_t	P
30 µm	0.44850	0.37521	2.14386
15 µm	0.44850	0.37521	1.28631
10 µm	0.44850	0.37521	1.07193
2.5 µm	0.44850	0.37521	0.42877

Predicted emissions ranges from 3.74 to 0.31 g/m2 at 8.2 m/s.

AP-42 Predicted Erosion Potential

8.4 m/s velocity (at 15 cm above surface)

z_o = 0.5 cm

u^*_t = 0.80677 m/s (with 6.86 m/s being the threshold velocity)

u^* = 0.98789 m/s (8.4 m/s)

	u^*	u^*_t	P
30 µm	0.988	0.80677	6.43550
15 µm	0.988	0.80677	3.86130
10 µm	0.988	0.80677	3.21775
2.5 µm	0.988	0.80677	1.28710

z_o = 0.1 cm

u^*_t = 0.54764 m/s (with 6.86 m/s being the threshold velocity)

u^* = 0.67057 m/s (8.4 m/s)

	u^*	u^*_t	P
30 µm	0.67057	0.54764	3.95007
15 µm	0.67057	0.54764	2.37004
10 µm	0.67057	0.54764	1.97503
2.5 µm	0.67057	0.54764	0.79001

z_o = 0.03 cm

u^*_t = 0.44154 m/s (with 6.86 m/s being the threshold velocity)

u^*_t = 0.54066 m/s (8.4 m/s)

	u^*	u^*_t	P
30 µm	0.54066	0.44154	3.04788
15 µm	0.54066	0.44154	1.82873
10 µm	0.54066	0.44154	1.52394
2.5 µm	0.54066	0.44154	0.60958

z_o = 0.01 cm

u^*_t = 0.37521 m/s (with 6.86 m/s being the threshold velocity)

u^* = 0.45944 m/s (8.4 m/s)

	u^*	u^*_t	P
30 µm	0.45944	0.37521	2.51728
15 µm	0.45944	0.37521	1.51037
10 µm	0.45944	0.37521	1.25864
2.5 µm	0.45944	0.37521	0.50346

Predicted emissions ranges from 4.69 to 0.96 g/m2 at 8.4 m/s.

Laboratory Experimental Results

30 μm =	0.438
15 μm =	0.180
10 μm =	0.111
2.5 μm =	0.040

Since the density of the particles are given, the above particle diameter has to be converted to aerodynamic diameter.

$d_a = d_{sedigraph} * (\rho_p)$^0.5

			% passing	
$d_{sedigraph30\ \mu m}$	=	16.360	20	(= 0.2)
$d_{sedigraph15\ \mu m}$	=	8.180	9.1	(= 0.091)
$d_{sedigraph10\ \mu m}$	=	5.453	6.4	(= 0.064)
$d_{sedigraph2.5\ \mu m}$	=	1.363	2.6	(= 0.026)

At 8.4 m/s, emission at time 0 is approximated to be 575 g/m2 at t=0.
% passing 200-sieve= 12.48 % 0.1248

30 μm particle erosion (da = 16.36) =	14.23 g/m2
15 μm particle erosion (da = 8.18) =	6.473 g/m2
10 μm particle erosion (da = 5.45) =	4.553 g/m2
2.5 μm particle erosion (da = 1.36) =	1.850 g/m2

At 8.2 m/s, emission at time 0 is approximated to be 255 g/m2 at t=0.
% passing 200-sieve= 12.48 % 0.1248

30 μm particle erosion (da = 16.36) =	6.440 g/m2
15 μm particle erosion (da = 8.18) =	2.930 g/m2
10 μm particle erosion (da = 5.45) =	2.061 g/m2
2.5 μm particle erosion (da = 1.36) =	0.837 g/m2

Measured laboratory emission ranges from 1.85 to 14.23 g/m2 at 8.4 m/s.
Measured laboratory emission ranges from 0.84 to 6.44 g/m2 at 8.2 m/s.

Micromeretics Laboratory Sedigraph Analysis

Particle Diameter (μm)	Percent Passing
120	99.8
110	99.6
100	99.1
90	98.0
80	95.8
70	92.0
60	85.5
50	75.5
40	61.8
30	43.8
25	34.8
20	26.2
15	18.0
12	13.6
10	11.1
8	8.9
6	6.8
5	6.0
4	5.3
3	4.5
2	3.5
1.5	2.8
1	2.1
0.8	1.7
0.6	1.2

VITA

Fook-Chi Soo was born in Petaling Jaya, Selangor, Malaysia on March 1, 1977. He attended high school in SRK Damansara Utama and consequently went on to attend college at Metropolitan College in January 1995. He then transferred to University of Tennessee in August 1996, to further pursue his Bachelors Degree in Civil Engineering. After graduating with a degree in Civil Engineering in December 1998, he went on to graduate school at the same university to pursue a Masters Degree in Environmental Engineering, where he received the degree of Master of Science in Environmental Engineering in July 2001.